ISTANBUL TECHNICAL UNIVERSITY ★ GRADUATE SCHOOL OF SCIENCE ENGINEERING AND TECHNOLOGY

INFLUENCE OF PISTON RING-PACK DESIGN ON INTER-RING PRESSURE OF A HEAVY DUTY DIESEL ENGINE

M.Sc. THESIS

Ahmet EBRİNÇ

Faculty of Mechanical Engineering

Automotive MSc Programme

MAY 2015

ISTANBUL TECHNICAL UNIVERSITY ★ GRADUATE SCHOOL OF SCIENCE ENGINEERING AND TECHNOLOGY

INFLUENCE OF PISTON RING-PACK DESIGN ON INTER-RING PRESSURE OF A HEAVY DUTY DIESEL ENGINE

M.Sc. THESIS

Ahmet EBRİNÇ
(503121701)

Faculty of Mechanical Engineering

Automotive MSc Programme

Thesis Advisor: Assoc. Prof. Dr. Özgen AKALIN

MAY 2015

İSTANBUL TEKNİK ÜNİVERSİTESİ ★ FEN BİLİMLERİ ENSTİTÜSÜ

BİR AĞIR HİZMET DİZEL MOTORUNDA PİSTON SEGMAN TAKIMI TASARIMININ SEGMANLAR ARASI BASINCA ETKİSİ

YÜKSEK LİSANS TEZİ

Ahmet EBRİNÇ
(503121701)

Makina Mühendisliği Anabilim Dalı

Otomotiv Yüksek Lisans Programı

Tez Danışmanı: Doç. Dr. Özgen AKALIN

MAYIS 2015

Ahmet Ebrinç, a **M.Sc.** student of ITU **Faculty of Mechanical Engineering, Automotive MSc Programme** student ID **503121701**, successfully defended the **thesis** entitled "**INFLUENCE OF PISTON RING-PACK DESIGN ON INTER-RING PRESSURE OF A HEAVY DUTY DIESEL ENGINE**", which he prepared after fulfilling the requirements specified in the associated legislations, before the jury whose signatures are below.

Thesis Advisor :	**Assoc. Prof. Dr. Özgen AKALIN** İstanbul Technical University	....
Jury Members :	**Assist. Prof. Dr. Hikmet ARSLAN** İstanbul Technical University	....
	Assoc. Prof. Dr. Muammer ÖZKAN Yıldız Technical University	....

Date of Submission : 04 May 2015
Date of Defense : 29 May 2015

FOREWORD

This thesis is written as a completion for the Automotive MSc programme in ITU Faculty of Mechanical Engineering. This thesis covers a mathematical model to predict the inter ring pressures for the determination of the influence of the piston/ring design parameters. The objective is to determine the critical parameters which are most effective on the second land pressures and to understand the effect of second land pressures on the engine tribological characteristics such as engine friction, wear and oil film thickness.

I would like to express my thankfulness to my advisor, Assoc. Prof. Dr. Özgen Akalın for his guidance during my study. I would like to thank my all colleagues in Ford Otosan, exclusively my supervisor Dr. Serdar Akça, Kaan Özdemir, Fatih Ünal and Özcan Gül for their continuing support and help.

A special thankfulness to my supervisor Dr. Serdar Akça and Nihan Çakır for their great encouragement and confidence in me in the difficult periods of my thesis.

Last but not least, I would like to present my gratitude to my family for their assistance, encouragement and love during my thesis and entire education life.

May 2015 Ahmet EBRİNÇ

TABLE OF CONTENTS

Page

ABBREVIATIONS

TDC **:** Top Dead Center
BDC **:** Bottom Dead Center
WOT **:** Wide Open Throttle
CO2 **:** Carbon dioxide

LIST OF TABLES

Page

LIST OF FIGURES

Page

SYMBOL LIST

A_m : End gap area of mth ring.
D : Cylinder bore diameter
F_{mass} : Force caused by mass of the ring
F_{fric} : Force caused by friction between ring and liner
F_{gas} : Force caused by the gas pressure
F_{bend} : Bending force
F_{hydr} : Damping force caused by oil filling of the groove
$F_{tension}$: Ring tension force
k : Adiabatic exponent
K_C : Orifice discharge coeffcient
K_i : Blow by parameter
$\dot{m}_{a_m}$: Gas flow through m^{th} ring gap
$\dot{m}_{b_m}$: Gas flow through m^{th} ring / liner clearance
$\dot{m}_{c_m}$: Gas flow through m^{th} ring / groove clearance
m_{in_m} : Total inlet gas flow to $(m+1)^{th}$ area
m_{out_m} : Total outlet gas flow from mth area
M_{gas} : Moment of gas
n : Engine speed
P_{above} : Gas pressure above the ring
P_{below} : Gas pressure below the ring
P_{behind} : Gas pressure behind the ring
P_{bottom} : Gas pressure on the bottom groove clearance
P_{top} : Gas pressure on the top groove clearance
P_r : Resulting gas pressure
P_m : Gas pressure between $(m-1)^{th}$ and mth ring
P_C : Critical pressure
P_{cr} : Crankcase pressure
R : Ideal gas constant
T_m : Gas temperature between $(m-1)^{th}$ and m^{th} ring
u : Potential energy
V_m : Volume of the space at m^{th} land.
v : Velocity of jet gas flow
δ_a : Clearance between ring and liner
δ_b : Clearance between ring and groove
θ : Crank angle
μ : Gas viscosity
ρ : Density of the gas
w : Crank angular velocity

INFLUENCE OF PISTON RING PACK DESIGN ON INTER-RING PRESSURE OF A HEAVY DUTY DIESEL ENGINE

SUMMARY

In today's circumstances, in order to meet the expectations of customers, OEMs are intended to produce engines with lower fuel consumptions without exceeding the legal emission limits but are pursued at the same time more powerful motors. In the purpose of this, any parameter that can lead to power loss in the produced engine is being examined in detailed and tried to be minimized. Even though it is possible to obtain any desired power from an engine, the durability and reliability of the engine component and the emission standards play a restricted role. In the light of all these expectations, the effect of the piston assembly which may be considered as the heart of an internal combustion engine can not be ignored.

In the open literature, there is a lot of work done in order to meet the above mentioned prospects. During this thesis, it will be focused on the pressure characteristics between the two rings which is considered as directly effective on the oil consumption and engine friction whereas indirectly effects on the fuel consumption. With the improvement of the pressure figures between two rings, the ring pack dynamics could be improved while the oil consumption, compression losses and friction are minimized to be able to take the emissions and fuel consumption under control.

The primary objective of a piston ring system is to seal the combustion gases during the engine process while minimizing the lube oil transported to the combustion chamber. So that the lube oil escapes past the rings can contribute the combustion process and increase the oil consumption by being burnt in the cylinder. Additionally, the compressed gas leakage through the rings and the increased engine friction can result a compression loss with reduced engine performance and increased fuel consumption. Because of all these reasons, the pressure characteristics between the two piston rings are considered to have a significant impact in the causes of above mentioned problems. For this purpose, it was decided to examine the effects of ring dynamics and behaviours on the second land pressure and friction for the Ford 9L Diesel 380 PS EU5 engine by modelling the pressure between the two rings. The main factor on the second land pressure is the amount of gas flow which escapes past the piston rings or ring grooves. For this reason, first of all the open literature has been investigated deeply in the view of used analytical methods. It has been seen that most widely used method is "Orifice and Volume Method" which also called as "Labyrinth Passage Way". In this method, the piston rings provide a labyrinth passages for the gases to leak out from the orifices while the gas flow is considered to be adiabatic and ideal gas. As the oil ring's sealing capability is negligible, the piston ring pack has been considered as two ring – one chamber passage system. By taking the boundary pressure conditions on the up and downside of the ring, the flow of the gas has been modelled and the second land pressure figures respect to crank

angle have been calculated with a computer code which has been written in MATLAB program.

As previously mentioned, in the allowed design rules, to be able to understand the effects of the design parameters on the second land pressure, some of the geometrical (ring gap width, ring thickness, piston second land area) and characteristic parameters (discharge coefficient) of piston and ring have been changed and the pressure values have been calculated in the MATLAB code again with a discussion of the results.

Finally, by using a statistical engineering method a DoE matrix has been created with Taguchi method to see the combined effect of the piston ring design parameters on the second land pressures. With this methodology, the most effective design parameters have been identified and according to the outcomes, the study was terminated by investigating the influence of second land pressures on engine friction, oil film thickness and power loss.

The outcomes from this study may contribute to the solution of the problems experienced during the design or aftermarket service phase of the engine development. With the useful information obtained from here can be used while questioning the design issues or considering the design changes.

BİR AĞIR HİZMET DİZEL MOTORUNDA PİSTON SEGMAN TAKIMI TASARIMININ SEGMANLAR ARASI BASINCA ETKİSİ

ÖZET

Günümüz koşullarında motorlu taşıt üreticileri yasal emisyon sınırlarını aşmadan müşterilerin beklentilerini karşılamak amacı ile daha düşük yakıt tüketimi olan fakat aynı zamanda daha yüksek güce sahip motorlar üretmek amacını gütmektedirler. Bu amaç doğrultusunda üretilecek motorlar içerisinde güç kayıplarına yol açabilecek herhangi bir parameter dikkat ile incelenmekte en aza indirilmeye çalışılmaktadır. Elektronik yakıt enjeksiyon sistemleri ile bir motordan istenilen gücü almak mümkün olsada, motor parçalarının dayanıklılığı ve emisyon standartları bu noktada kısıtlayacı rol oynamaktadır. Bütün bu beklentilerin ışığında, bir içten yanmalı motorun yaşam kaynağı olarak adlandırılabilecek piston grubunun etkisi göz ardı edilemez büyüklüktedir.

Açık literatürde, beklentileri karşılayabilmek adına yapılmış bir çok çalışma mevcuttur. Bu tez boyunca yağ tüketimine ve sürtünmeye direk etkisi, yakıt tüketimine dolaylı etkisi olduğu düşünülen iki segman arası basınç karakteristiği üzerinde durulacaktır. Segmanlar arası basınç değerleri optimize edilerek segman dinamiği iyileştirilebilirken, aynı zamanda yağ tüketimi, sıkıştırma kayıpları ve sürtünmeler en aza indirilerek emisyon değerleri ve yakıt tüketimi kontrol altına alınabilir.

Bir piston segman grubunun başlıca görevlerinden birisi sıkıştırma işlemi sırasında yüksek basınçtaki taze dolgu için sızdırmazlık sağlarken, yanma odasına kaçabilecek motor yağını minimize etmektir. Öyle ki segmanlar arasından geçerek silindire kaçan yağlar, silindir içerisinde yanarak yağ tüketimini artırırken, yine segmanlar arasından motor karterine kaçan sıkışmış gazlar ve artan sürtünme kuvveti yanma ve motor performansını düşürürken yakıt tüketimini artırıcı yönde etkide bulunabilir.

Emme işlemi sırasında silindire giren hava, özellikle günümüzde aşırı doldurmalı motorların kullanılmaya başlanması ile sıkıştırma işlemi sırasında çok yüksek basınçlara ulaşmaktadır. Bu esnada piston sistemi sıkıştırılan bu havayı silindir içerisinde tutarak karter bölgesine kaçmasını engellemek ile görevlidir. Yanma işlemine katılacak havanın silindirden kaçarak karter bölgesine kaçması silindire giren toplam hava miktarını düşürmek suretiyle yanma verimini düşürmekte, emisyonları ise artırmaktadır. Ayrıca gerekli maksimum silindir basıncına ulaşamamak suretiyle piston üzerine etkiyen kuvvetler azalarak motorda güç kaybına yol açmaktadır.

Karter bölgesinde bulunan yağ motor çalışma noktasına göre yüksek sıcaklıklara ulaşabilmektedir. Piston segmanlarından ve silindirden aşağıya kaça gazlar bu bölgede buharlaşma sonucu açığa çıkan yağ buharı ve karterdeki yağ ile birleşmektedirler. Geçmişte bu gazlar dışarıya atılırken, günümüz motorlarında çevre temizliği kısıtlamaları uyarınca bu gazlar içerilerindeki yağ buharı süzülerek

tekrardan yanmaya katılması için silindir içerisine gönderilmektedir. Öte yandan süzülen yağ buharının damlacıklar halinde kartere geri gönderilmesi hedeflenir. Pratikte bu yağın tamamen süzülmesi mümkün olmamakta ve silindir içerisine geri gönderilen hava içerisinde kalan yağ damlacıkları yanmaya katılarak yağ tüketimini ve emisyonları artırıcı yönde etkide bulunmaktadır.

Motor karter bölgesindeki veya silindir yüzeyinde kalan yağlama yağının silindir içerisine kaçarak yanma işlemine katılması sonucu içten yanmalı bir motorun yağ tüketimi artış göstermektedir. Günümüz şartlarında özellikle ağır ticari vasıtalarda yüksek yağ tüketimi istenmeyen bir durumdur. Zira yağ servis aralığı düşük olan araçlar sık sık servis edilmek zorunda kalmakta ve müşteriye ekstra maliyet olarak yansımaktadır. Ayrıca taşımacılık sektöründe araçların servislerde geçirdiği süre, işletmeciye iş kaybı olarak geri dönmektedir. Buna ek olarak motor yağının yanmaya katılması yanma verimini düşürürken zararlı egzoz emisyonlarını artırıcı yönde etki yapmaktadır.Ayrıca kötü yanma sonucu biriken karbon parçaçıkları piston ve segmanları olumsuz yönde etkileyerek, ciddi motor arızalarına yol açabilmektedir.

Günümüz taşıt üreticileri müşteriden gelen talepler doğrultusunda tüketilen yakıt miktarını düşürmek üzere çalışmalarını yoğunlaştırmışlardır. Bir motorun yakıt tüketimi o motorun çalışma verimi ile doğrudan ilgili olup kaybedilen enerji miktarı ile doğru orantılı olarak artış göstermektedir. Bu yüzden sürtünme kayıpları en aza indirgenerek aynı yakıt miktarı ile daha fazla güç alınması mümkündür. Bu yöntem ile yanma verimi artırılırak her geçen gün katılaşan emisyon düzenlemelerine uyum sağlanabilmektedir. Ayrıca sürtünmenin parçalar üzerindeki aşındırıcı etkisi azaltılarak genel motor ömrünün uzatılması mümkün olmaktadır.

Bir içten yanmalı motorda sürtünme kaynaklı enerji kayıplarının neredeyse yarıya yakını piston,segman ve silindir sisteminden kaynaklanmaktadır. Özellikle üst ölü noktada birinci kompresyon segman bölgesinde taşınan yağ miktarının düşük olması sebebiyle burada iki metal yüzey arasında bir temas gerçekleşmekte ve buna paralel olarak sürtünme kayıpları ve aşınmalar ortaya çıkmaktadır. Bu noktada segman ve silindir arasında oluşan minimum yağ film kalınlığının etkisi önem arz etmektedir. Birinci ve ikinci segman arasındaki hacimde oluşan basınç değeri iki yüzey arasındaki yağlama rejimi ve yağ film kalınlığını belirlerken sonuç olarak da oluşan sürtünme kuvvetinin değerini değiştirmektedir.

Bütün bu sebeplerden ötürü, iki segman arasındaki basınç karakteristiği yukarıda sayılan problemlerin nedenleri içerisinde önemli bir etkiye sahiptir. Bu amaçla Ford 9L Dizel 380 PS EU5 motoru için iki segman arası basınç modellemesi yapılarak, segman karakteristiklerinin basınç ve sürtünme üzerindeki etkisinin incelenmesine karar verilmiştir.

Öncelikle, derin bir literatür çalışması yapılarak geçmişten günümüze kadar iki segman arası basınç karakteristiklerinin incelendiği yayınlar ve makaleler analiz edilerek, yapılacak çalışmaya neler katılabileceği üzerinde fikir yürütülmüştür. Literatür araştırmaları sonucunda iki segman arasındaki basıncın dayandığı temel faktörün, segman boşluklarından yada segman yuvalarından aşağıya kaçan gaz akış miktarı olduğu görülmüştür.. Bu sebep ile açık literatür taraması yapılarak analitik hesaplama metodları araştırılmıştır. Çoğunlukla kullanılan yöntemin “Orifis – Hacim” metodu olduğu görülmüştür. Aynı metod piston segmanlarını gazlar için labirent şeklinde bir geçiş yolu sağladığı için “Labirent Geçiş Yollu” metodu olarak da adlandırılır. Bu yöntemde hacimler arası gaz geçişi adyabatik ve ideal gaz olarak kabul edilerek, dörtgen kesitli orifisler vasıtası ile gerçekleştiği düşünülmüştür. Yağ segmanının sızdırmazlık özelliği ihmal edilebilir derecede olduğu için, system iki segman – bir hacim olarak kabul edilmiştir.

Yapılan çalışmanın ana amacı doğrultusunda matematiksel modeli basitleştirebilme adına piston ikincil hareketi ihmal edilmiştir. Sınır koşullarını belirleyen segman alt – üst bölgesindeki basınç değerleri de hesaba katılarak gaz akışı modellenmiş, MATLAB programında yazılan bir kod yardımı ile Euler iterasyon metodu kullanılarak çözdürülmüş ve krank açısına bağlı olarak iki segman arası basınç değerleri hesaplatılmıştır. Elde edilen sonuçlar daha önceden AVL Glide programında yapılan simülasyon verileri ile karşılaştırılarak yakın sonuçlar elde edildiği gözlemlenmiştir.

Daha önceden de bahsedildiği üzere, segman tasarım parametrelerinin iki segman arasındaki basınca etkisini gözlemlemek adına tasarım sınırları içerisinde kalacak şekilde, birinci ve ikinci segman boşluk genişlikleri, birinci ve ikinci segman yükseklikeri, birinci ve ikinci segman arası piston yüksekliği, akış tahliye katsayısısı ve birinci segman ile silindir duvarı arası mesafesi gibi geometrik ve karakteristik parametreler değiştirilerek oluşturulan MATLAB kodunda tekrar çözümleme yapılarak etkileri yorumlanmıştır.

Son olarak istatiksel mühendislik yöntemlerinden yararlanılarak Taguchi metodu ile bir DoE matrisi oluşturulmuş, segman dizayn parametrelerinin birlikte olan etkileri araştırılmıştır. Bu yöntemde seviye ve parameter sayısına göre matris tipi belirlenmekte ve test edilebilecek tüm varyasyonlar elde edilebilmektedir. Oluşturulan DoE matrisinde yer alan piston segman tasarım parametrelerine göre 8 farklı simülasyon oluşturulan MATLAB kodunda koşturularak yeni segmanlar arası basınç değerleri elde edilmiştir. Tasarım parametrelerinin minimum ve maksimum ölçülerde iken ayrı ayrı ortalama segmanlar arası basınçları hesaplanarak her bir parametrenin etkisi grafik üzerinde gösterilebilmektedir.

Hassasiyet analizi sırasında test edilen 8 piston segman grubundan üç farklı segman konfigürasyonu belirlenerek, elde edilen birinci ve ikinci segman arasındaki basınç değerleri sürtünme analizi için kullanılan ikinci bir MATLAB kodunda girdi olarak kullanılmıştır. Yapılan sürtünme analizi sonucunda segmanlar arası basınç büyüklüğünün birinci segman özelinde yağ film kalınlıkları, yağ film kavitasyon noktası, yağ filmi basıncı, toplam sürtünme kuvveti ve enerji kayıpları üzerindeki etkileri incelenerek, yağ tüketimi ve motor aşınmaları üzerine yorumlar yapılmıştır.

Bu çalışma sonucunda elde edilen çıktılar, motor geliştirme yada satış sonrası safhada ortaya çıkabilecek problemlerin ön görümünde veya araştırılmasında faydalı bilgiler sağlayarak yapılabilecek tasarım değişiklikleri ile çözümüne katkı sağlayabilecektir.

1. INTRODUCTION

1.1 Motivation

Nowadays, in the world of automotive industry, more powerful engines with lower fuel consumption is one of the mostly demanded item for the internal combustion engine manufacturers and developers due to customer requirements. From the point of customers, this can be formulated easily but for the developers it could be more sophisticated with so many parameters included such as engine friction, cylinder kit performance, emissions, oil consumption and blow by.

For the required engine performance characteristics, understanding the cylinder kit dynamics is a key item to specify the parameters which will cause engine performance loss. Inter ring pressure is one of the most important parameter for the control of oil consumption, emissions and reduced engine friction. There are several studies available which investigates the ring motion via inter ring pressures and effects on the blow by and oil consumption; this thesis focuses on the changes of the inter ring pressures by the piston ring pack dynamics and influences on the piston friction.

Through the rings positioned around the piston inside the ring grooves, the piston system aims to seal, as much as possible, both the combustion gases and engine oil. Combustion gasses located on top of the piston must be restricted to reach the crankcase region below the cylinders; whereas the engine oil must be restricted to get in contact with combustion. The gasses that leak from the cylinder cause increase in “blow-by”, whereas some of the oil that reach the cylinders burn and cause oil consumption.

1.2 Literature Review

A number of significant studies have been presented over years for the prediction and measurement of the inter ring gas pressures with different methods and their effects on the engine characteristics such as cylinder kit wear, ring axial motion, oil consumption and blow by.

Ting and Mayer (1974) from Ford Motor Co. developed a method for computing the inter ring pressure variations during the cycle for a general piston ring pack. It has been assumed that piston rings provide a passage way for the gases to escape the piston through the ring gaps which decided as an only open area to leak out and represent the ring by a passage system consists of series of chambers with square edged orifices. This “Labyrinth Passage Way” has been a milestone for the further developers in their studies. As a result of this study, the calculated pressure distributions above and below the ring have been used as boundary conditions during the calculation of oil film thickness. On the other hand, it had been possible to obtain the amount of leaked gases into the crankcase for the calculation of blow by figures of the engine [1] [2].

Rudy et al. (1983) from Institute of Tribology, University of Leeds, established an extended orifice and volume method for predicting the gas pressures between the piston rings to be able to take account of the energy loss due to cylinder wall friction in the circumferential gas flow between the piston and liner. With the aim of this, instead of using a complex three dimensional gas dynamic analysis, an elementary one-dimensional theory has been developed to be able to use in conjunction with the previous orifice and volume methods. The theoretical analyses have been performed at Leeds for over twenty large bore diesel marine engines. Three different type engines have been investigated to see the influence of circumferential gas flow upon the calculated inter ring pressures. It has been found that in two-stroke single cylinder engine with 0.17 m cylinder bore, such flows had a negligible effect. In opposite it has been seen a visible effect on the 4-stroke marine engine with 0.5 m cylinder bore especially under worn conditions due to pressure losses incurred by the gas as it flows around the piston to reduce the rate at which the gas can pass through the first ring end gap to the second land. The general results suggest that circumferential gas flow is significant only when the mass flow rates within a ring pack exceed 10^{-2} kg/s which the ring wear can majorly increase the size of the ring end gaps. Additionally the experimental data that has been conducted in this study showed that including the additional volumes in the calculations due to ring groove clearances provides a better correlation with the analyses results [3].

Liu and Yongzhang (1986) from Purdue University, used the same "Labyrinth Passage Way" method during the prediction of the sealing characteristics of piston rings of a reciprocating compressor with the implementation of the flow rates between the ring and cylinder bore and the ring and its groove by using the Navier Stokes equations and considering the oil sealing effect [4].

Richardson (1996) from Cummins Engine Co. studied the pressure distributions in a six-cylinder engine that the experimental work has been performed in 1991. For the dyno testing, an instrumented piston with a pressure transducer mounted on the second land and a cylinder head with a pressure transducer have been used. To be able to bring the wires outside the piston "Grass-hopper" linkage system has been used. During this study, it has been investigated the effects of the ring twist on the inter ring pressures and found out that a negative twist of a second ring can cause significant changes on the ring motion and inter ring pressure with an increased blow by [5].

Tian et al. (1997) from MIT analyzed the wear patterns of the rings and grooves of a diesel engine. They used a ring dynamics/gas flow model with a ring-pack oil film thickness model. The new and worn engine's ring/groove and ring/liner contact has been analyzed, and the effects of ring dynamics on the oil transport and oil consumption have been investigated. It has been concluded that the negative static twist on the second ring can result in ring flutter during the late part of the compression and early part of the expansion strokes as the gas is blown down through the second ring/groove clearance and the second land pressure is also dropped although it is also beneficial for the oil consumption control [6].

Richardson and Chen (2000) from Federal Mogul Corp., evaluated overall six different commercial or university developed cylinder kit dynamics models which was used for the prediction of the power cylinder system performance and presented the results from only one of these programs. Two sets of results were generated which the first one is without any calibration work, the other one is by changing only one parameter regarding the engine running conditions. The results have been verified with an experimental work by performing a telemetry test to be able to measure the blow by, actual inter-ring pressure on the second land and the ring motion on the top and second rings. The results showed that the predictions were better with the improved model rather than the first iteration without any calibration work, however the blow by comparison between model and experimental results showed very different behaviors which can be related with a problem about sealing of the engine as with a linkage system usage, it can result poor engine sealing. Also the model could not predict the ring fluttering which will affect the inter-ring pressures significantly. It has been concluded that due to incorrect predictions of ring motion and its direct effects on the land pressures, the actual and predicted inter-ring pressure results did not show a good correlation [7].

Herbst and Priebsch (2000) from AVL List GmbH, developed a piston ring dynamics model for axial motion, inter ring pressures and oil consumption by using AVL Glide Software with a comparison of 2 different ring configuration regarding different ring end clearances for top and second ring. The inter ring pressure calculation is based on labyrinth passage way by extending it with the orifices addition to the groove and liner areas. The predicted inter ring gas pressure figures showed a good correlation with the measurement results. Then this pressure figures have been used for modeling the hydrodynamic lubrication between the ring running face and liner wall for the evaluation of the oil consumption [8].

Richardson and Krause (2000) from Cummins Engine Company, studied two different engine with a low oil consumption while the ring motion and gas flows through the ring packs are significantly different regarding the effects of the cylinder kit wear on the blow by and oil consumption as a result of changing inter-ring pressures. To evaluate the cylinder kit dynamics, Ricardo RINGPAK software has been used. With a new engine, the gas pressure build up on the second land vents upward around the back of the top ring rather than downward which past the second ring which will decrease the blow-by. However, since the wear increases on the top ring face and liner, the ring pack dynamics will change and with the increasing of the second land pressures gas flow from second land into the combustion chamber will increase and this blow back carries the oil into the combustion chamber that results increasing oil consumption with the burning of the oil. In addition to this, this study has showed that a good sealing capability of second ring is related with the stability of the second ring motion as the lifting of second ring can cause a drop in inter-ring pressures. The study has been concluded that, the top ring wear is significantly effective on the oil consumption due to blow back because of the higher inter-ring pressures. On the other hand, the second ring wear is most effected on the blow by as the gas flow are through the second ring increases which results downward flow will increase [9].

Tamminen et al. (2005) from Helsinki University of Technology, presented a work aims to determine the gas pressure acting on the ring pack for a medium speed diesel engine. Experimental work has been done with an instrumented piston via telemetric data transmission. The measurement results have been verified with the computer simulation results by the Ricardo RINGPAK Software. Furthermore, the effect of piston running clearance and the ring face wear effects on the inter ring pressure has been investigated. It has been concluded that an increased piston-liner clearance will increase the land pressures due to increased ring end gap. In addition, the study showed that for a good sealing capability of the ring, the second land pressure should be lower than the pressure behind the first ring [10].

Mittler et al. (2009) from Federal Mogul Corp. developed a mathematical code to describe the physical basics of ring movement under dynamic loading conditions which was verified with a telemetry testing on the dynamometer by measuring the actual ring motion and inter-ring pressures. A simplified mathematical model has been used to evaluate the point where the piston ring starts to move and the results of the calculation of the pressure in the top and bottom clearance showed that the axial gas force and gas moment are independent of the pressure behind the ring. In the next stage, the model has been detailed with the derivation of the mathematical model by taking the change of curvature and torsion, gas dynamics in the clearances and choked flow by friction into account. The results that was obtained by comprising the measurements and calculations showed that the effects of ring movement and twist are much more instructive by theoretical inspection rather than by detailed engine measurements [11].

1.3 Objective

The background and literature survey above showed that the piston ring dynamics is very critical parameter to be able to define the piston ring pack characteristics due its effects on the ring motion and inter ring pressures. Besides this, inter ring pressures are also effective on the engine critical parameters such as oil consumption, blow by, engine friction and engine wear.

The background of the piston-ring dynamics showed that the pressures between the two ring spaces are clearly dependent on the gas mass flows from the opening areas of piston-ring-liner to the land areas. The review of the literature clearly indicated that the other researchers had predicted the inter ring pressures by using the "Labyrinth Passage Way" for modeling the gas flows which shown in Figure 1.1 for an entire ring package by applying the Ideal Gas Laws.

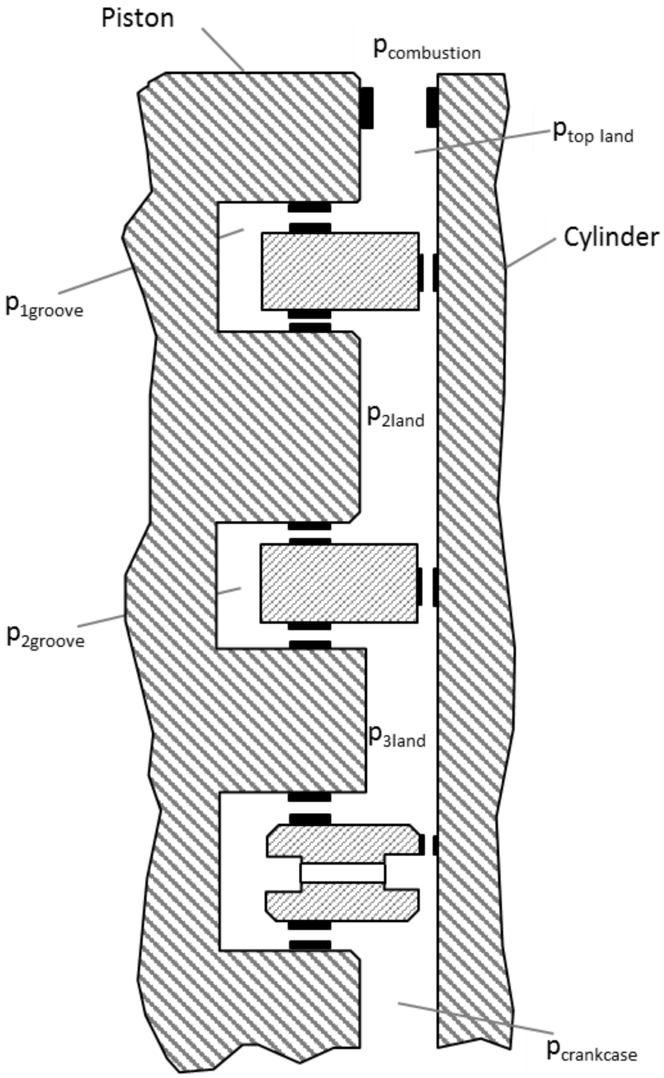

Figure 1.1 : Labyrinth Passage Way [15].

The objective of this thesis is to develop a mathematical model for a 9L Ford ECOTORQ Heavy Duty Diesel Truck engine to determine the gas pressure distribution between the rings and to see the effects of different ring pack configurations on the inter ring pressures by changing some of design parameters. While modeling the gas mass flows through the piston rings, "Labyrinth Passage Way" method will be used with orifices that gave reasonable results in previous studies. With the mathematical formulas, which will be shown later, a computer code has been written in MATLAB and the related crank angle dependent differential equations were solved by using Euler Iteration Method. Furthermore, with the aim of investigating the effect of ring pack behavior on second land pressures, a DoE matrix has been established via Taguchi Method. The experiments have been run by changing some of piston ring design parameters such as piston ring end gap area, piston running clearances, piston ring thickness, piston second land height etc. by giving a minimum and maximum value. With the results that obtained from DoE experiments, three different ring pack configurations have been chosen for the piston ring tribological analysis to investigate the second land pressure effect on the friction force, oil film thickness and wear. During this analysis another computational scheme has been used which was developed and verified by Akalin and Newaz (2001) for the friction modeling of a piston ring – cylinder bore in mixed lubrication regime [22].

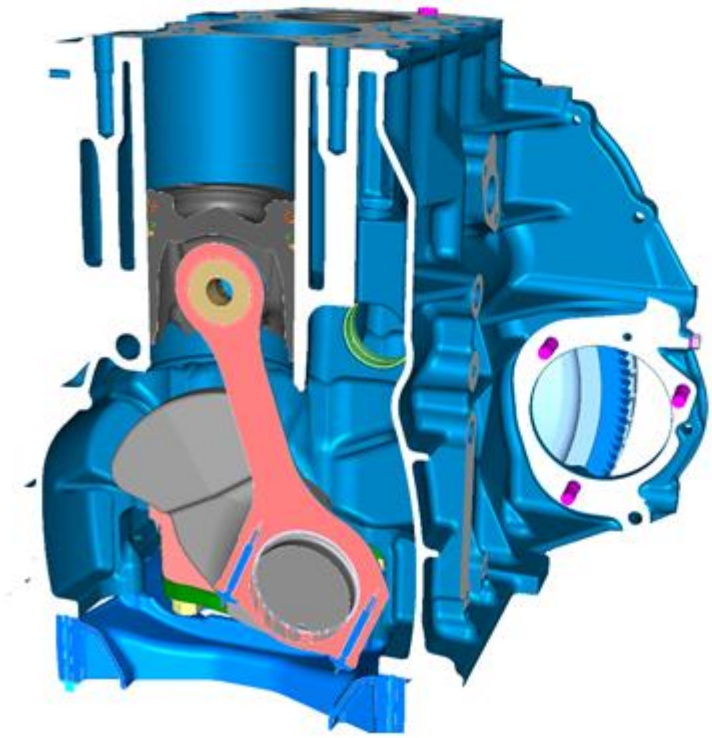

Figure 1.2 : Power Conversion System of 9.0L Heavy Duty Diesel Engine.

2. GENERAL REMARKS

2.1 Pressure Distribution Between the Piston Rings

The primary objective of the piston-ring system is to seal the combustion gases and the engine oil. Not to cause an increase in the blow by and loss of engine performance, it should not be let the gases reach to the crankcase area with a good sealing capability of piston rings. On the other way, the engine oil needs to be operated between the piston and liner uniformly not the combustion chamber. Poor oil sealing capability of the piston rings will lead the engine oil to be mixed with combustion gases, which will result in cylinder burning and increased oil consumption.

It is considered that the pressure distribution between the piston rings is one of the most important parameter that will affect the oil consumption and blow by figures of an engine with the motion of the ring due to pressure differences. In a cylinder, the direction of a gas leakage through the piston rings is depends on the pressure figures between piston rings with respect to the combustion pressure. Any changes in the inter ring pressure will result the ring to be fluttered, collapsed or twisting during the engine operation. These all ring motions may cause the oil to be thrown off to the cylinder or gas leakages to the crankcase area, which will result increase of the oil consumption and blow by values of an engine.

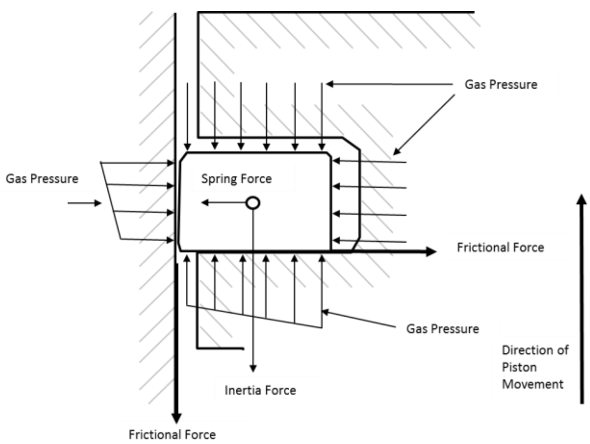

Figure 2.1 : Typical forces acting on a ring.

2.1.1 Ring Flutter

Although the piston rings form a reliable sealing between the cylinder and bore, there is a particular case where piston rings can cause a problem owing to a vibration condition, which is due to combination of factors centered around the fundamental geometry of the engine, the mass of the piston rings, engine speed and pressure differential across the piston rings. The ring flutter is considered to be caused by pressure that leaks by the top ring but does not get by second ring. The load distribution and orientation depends both on the radial pressure of the ring and its distribution and on the pressure from combustion that builds up in front of and behind the ring.

During the movement of the piston to the bottom dead center in the exhaust stroke, the forces acting on the ring owing to pressure differential and inertia push the ring up against the top side of the groove. As the speed of the engine increases, the piston acceleration increases as the square of the engine speed. So even in a small increase in maximum engine speed, it will cause the onset of the ring flutter.

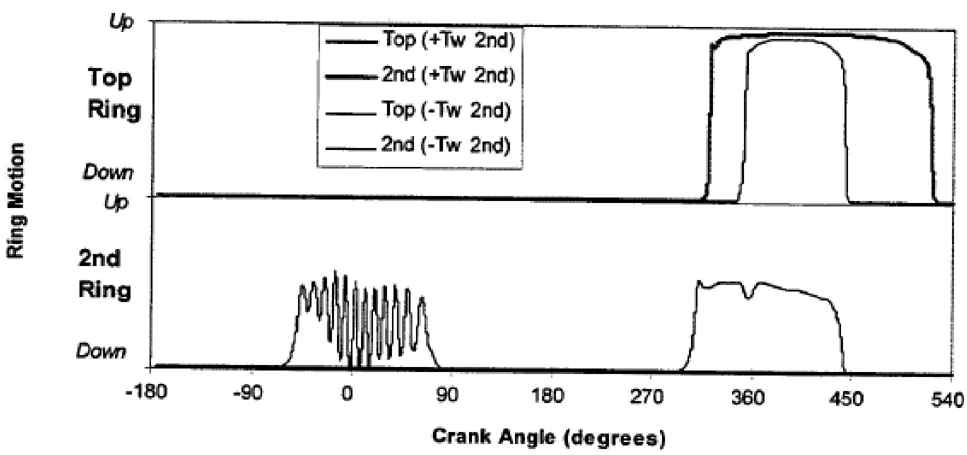

Figure 2.2 : Graph showing the ring flutter [5].

2.1.2 Ring Collapse

A piston ring collapses radially when a positive load differential oriented radially inwards is present between the outer and inner diameter of the ring that exceeds the ring tension. The second ring in high-speed engine operation contacts with the ring groove upper surface around the compression top dead center due to inertia of the ring itself. The second ring in such a state is subject to a force pushing the ring against the cylinder wall due to pressure applied to the back surface of the ring and the surface pressure of the ring caused by tangential force of the ring itself [24].

On the other hand, there are some forces to pull of the second ring from cylinder wall due to second land pressure and third land pressure on the outer circumference of the piston ring. This phenomenon – the ring pushed into its groove and loss of its sealing function on the circumference- is called as ring collapse.

2.1.3 Ring Twist

To be able to control the oil consumption and blow by, a relative twist angle can be given to the piston ring by using of a chamfer on it. This could be explained by the balance of moments. Depending on the chamfer location, one side of the ring will lift due to a higher moment figures. There are non-twist, positive twist and negative twist. For the top rings, non-twist or positive twist rings are used for the control of the blow by while the negative twist rings are used rarely. On the other hand, negative twist rings are generally used for second rings for the control of oil consumption by preventing the oil throw off to the combustion chamber.

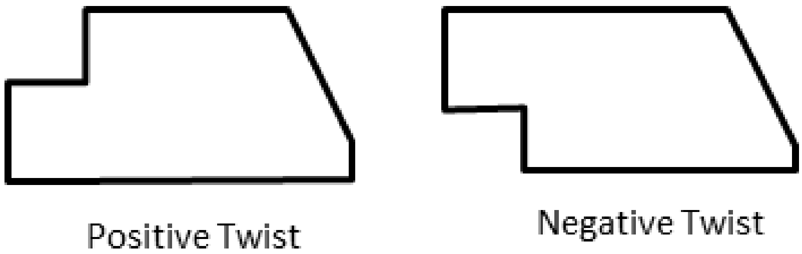

Figure 2.3 : Twist angles of a piston ring.

Twisting of a piston ring is only effective when there is no combustion pressure acting on the ring as during the engine operation once the combustion pressure reached to the ring groove, the piston ring is pressed flat onto the lower groove side that can improve the oil consumption [13].

With a positive twist ring even it presents an effective oil scrapping behavior, the ring may lift off the lower groove side that allows the oil enter into the sealing gap and thus contributing to the oil consumption.

With a negative twist ring, sealing of the ring groove at the outer lower ring flank and at the inner upper flank will prevent the oil to enter into the groove, thus effects the oil consumption positively.

2.2 Engine Friction

An internal combustion engine has too many dynamic components that produce friction. While some of these friction forces remain stable due to constant applied loads, some of them alter with the increasing of the engine speed. The frictional process in an engine can be expressed in three categories:

- the mechanical friction, which includes friction caused by the relative motion of internal moving parts such as crankshaft, piston rings or valve train.
- the pumping work, that is the work done during the intake and exhaust strokes by air filter, throttle, valves or after treatment exhaust systems to move the working fluid through the engine.
- the accessory work, which is required for the operation of oil pump, fuel pump or water pump.

The studies done in 2000s confirm the piston system has the largest contribution with about 50% to the mechanical losses that caused by friction whereas the journal bearings take the second place with about 30% [14].

The distribution of the mechanical losses can be seen in Figure 2.4.

While the bearings are fully lubricated without metal - metal contact, some parts of the piston assembly experience metal -metal contact most of the time under the high loads. Since the oil film is weak around the top of the piston, first compression ring is exposed to metal - metal contact every time when it passes the TDC. On the other hand, the running surfaces of the rings and especially the skirt of the piston are also in contact with the cylinder liner that is considered as the main source of the engine friction.

The mechanical losses which caused by the engine friction are also effective on many engine parameters like fuel consumption, engine performance and emissions. By reducing the friction, the performance of the engine will increase with a more efficient combustion while the fuel consumption and CO_2 emissions are decreased. Beside this, less wear because of low friction, the service life and the durability of the engine components will be extended and improved.

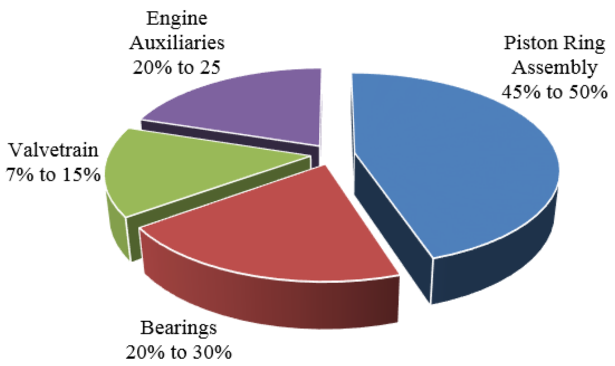

Figure 2.4 : Distribution of the total mechanical losses of a diesel engine [14].

2.3 Engine Wear

With the stricter emission legislations and higher power demands from the customers, the durability and the reliability of the components of an engine are strictly required. As a result of increased combustion pressures and engine friction, the wear levels on the engine parts are being increased day by day. The engine wear can be described as a material removal from a surface due to a contact between two mating surfaces. Mostly observed wear types are shown as below:

- **Adhesive wear:** Large plastic deformation due to relative motion creates the wear debris and material transfer from one surface to another. It generally occurs when the two bodies slide over or are pressed into each other in the contact region under compression and shearing.

- **Abrasive wear:** Loss of material due to a rough or hard surface slides across a softer surface with hard particles embedded in the surface softer material. It is commonly classified as two-body and three-body abrasive wear according to their type of contact and the environment of the contact.

- **Corrosive wear:** This type of wear can be described as a material degradation due to corrosion and mechanical sliding action. Corrosive wear is the result of acids and chemicals that are commonly produced in the combustion process that is highly effective on the corrosion levels of cast iron cylinders and piston rings [19].

- **Fatigue Wear:** Surface fatigue is a process that is produced due to repeated sliding or rolling and cycling loading. It will result with an initiation of crack on the components and depends on the properties of material and stress pattern, the crack can be grown and a material loss may occur by leaving a hole or pit [19].

- **Scuffing:** This type of wear can also be considered as severe adhesive wear that occurs in highly loaded lubricated areas such as piston rings. With the breaking of the oil film between the two surfaces, metal-metal contact starts and remove the material at each subsequent contact that can lead to noisy and catastrophic engine failures within minutes.

2.4 Oil Consumption

The lube oil is one of the most important fluids for an engine which provides the lubrication to reduce the friction, cooling on some engine components and protection against the corrosion. In the light of these features, the oil consumption is a parameter that states the total life of the engine with a determination factor while defining the oil service intervals as decreasing the oil consumption will mean longer oil service intervals for the heavy duty commercial vehicles. In an internal combustion engine, most common oil consumption mechanisms can be described briefly for the piston-ring-liner system as below:

- **Evaporation:** During the high load - hot running conditions, engine components' thermal loading gets higher due to convectional heat transfer between the combustion chamber and cylinder wall. With the effect of the heat that discharged to the liner, the remaining oil on the surface of cylinder wall starts to evaporate and mixed into the combustion gases. This will contribute to the total oil consumption as the oil leaves the engine in burnt or unburnt state by joining the combustion process.

- **Throw off above the top ring:** Due to inertial forces caused by the acceleration and deceleration of piston assembly, accumulated liquid oil above the top ring can be transported into the combustion chamber. The amount of oil is being defined by the oil scrapping of top ring, oil flow at ring/groove sides and oil flow through the ring end gap to the piston second land [15].

- **Reverse Oil Blow through top ring:** When the pressure gradient on the top ring is negative which means second land pressure is greater than the combustion pressure, the mist oil in the gases will flow into the combustion chamber through the top ring end gap. Additionally, in case of any instability of the top ring due to ring flutter, some oil can pass around the top ring groove and contribute to the combustion process.

- **Entrainment in Blow By:** Piston ring end gap, bore distortion or other reasons can lead some gases coming from the combustion chamber to move the engine crankcase during the compression stroke. During the transport of the blow by gases, lubrication oil can absorb into the gases by atomization of the film or evaporation of oil under high gas temperatures. Even with the crankcase ventilation systems, this amount of oil is tried to be separated and sent back into the oil sump again, in any case, some of oil mist remains in the air and sent back to the intake manifold to rejoin the combustion process [16].
- **Oil scraping of piston top land edge:** With the effect of piston tilt, secondary motion of the piston and any dirt on the top land, the piston top land can contact with the cylinder wall. As a result of this, the oil will be scraped by the piston top edge at each upward stroke and pushed against the top deck [8].

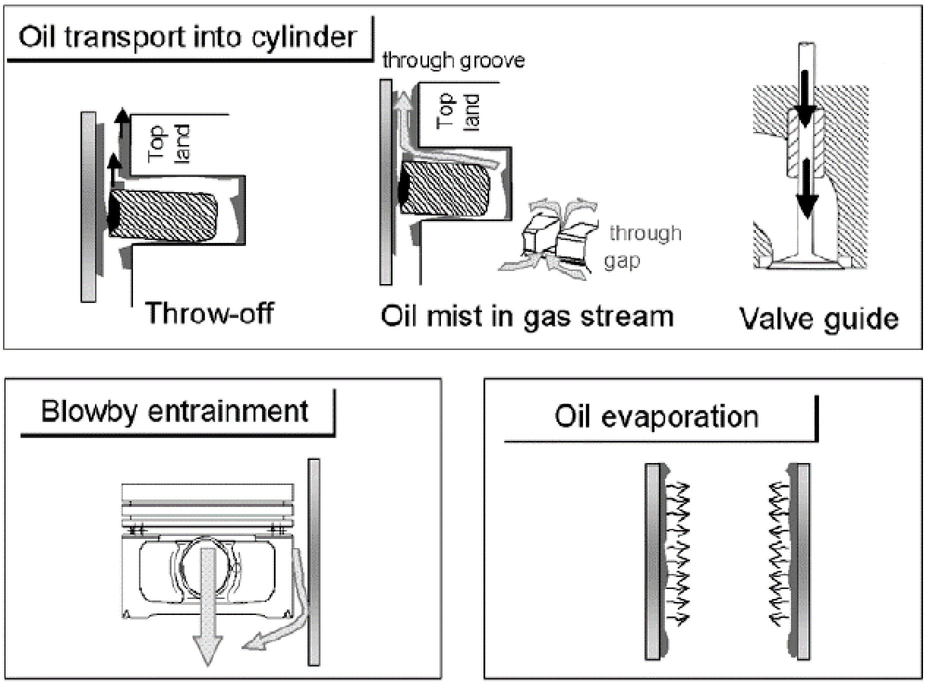

Figure 2.5 : Oil consumption mechanisms [17].

The other important effect of the oil consumption is on the engine combustion characteristics. Burning some of the oil in the cylinder during the combustion phase may increase the performance unintentionally but in the point of poor combustion quality, this will affect the emissions in a negative way due to the by-products of combustion. The main factors affect the oil consumption figure are shown as below:

- Loss of sealing capacity of the impeller due to worn bearings of the turbocharger.
- Fuel / oil mixture injection into the combustion chamber due to worn fuel injection pump
- Oil escaping into the intake system due to loss of CCV performance
- Worn valve stem seals and valve guides due to excessive wear or installation error
- Cylinder head distortions due to installation errors.
- Loss of sealing capacity of the piston rings due to wear, or incorrect installation
- Fuel/oil mixture due cylinder bore fuel flooding after an injection fault
- Increased wear levels on the power conversion system parts due to irregular maintenance, low-quality mineral oils, cylinder distortion and machining faults during drilling and honing [12].

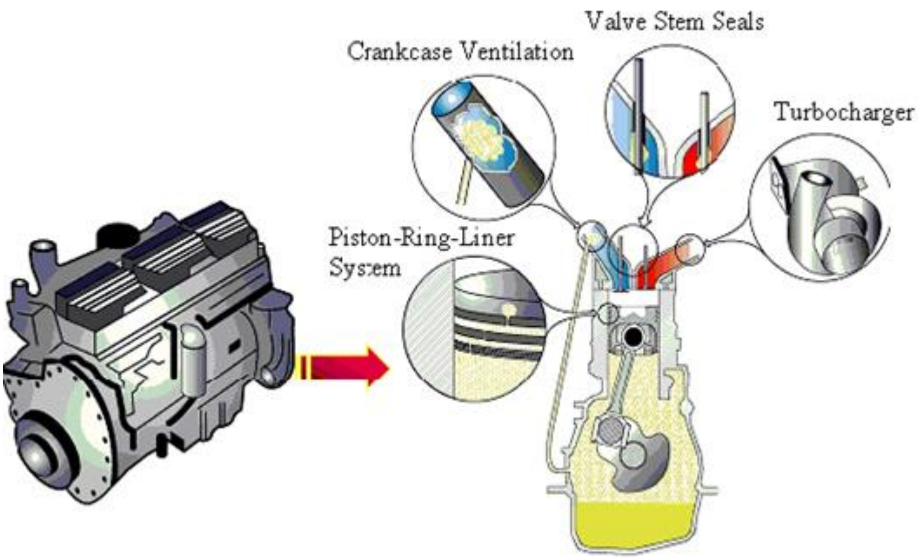

Figure 2.6 : Oil consumption sources [18].

2.5 Blow By

During the engine running, there is a compressed air and fuel mixture inside the combustion chamber which is exploded and forces the piston down. However, some of the mixture can go through the crankcase area by passing the piston rings that is responsible to seal the gaps between cylinder wall and the piston. The piston rings in an internal combustion engine achieve efficient sealing with both the cylinder wall in a radial direction and the top or bottom sides of the piston ring grooves in an axial direction. The contact pressure on the cylinder wall is achieved by the inherent spring force of the ring with the gas pressure behind the ring. On the other hand, the axial forces which composed of the gas pressure above and under the ring, the mass forces and the friction forces provide the contact on the side of the piston ring groove. Since these forces change their direction during the cycle, the ring moves from one side to another during the cycle. In these cases, the piston ring can no longer create a seal against the ring groove flank and the combustion gas can pass around the back of the piston ring that has a significant effect on the blow by.

As the cylinder pressure increases in the combustion chamber, the gases that escape around the piston causes a decrease in the cylinder pressure that effects the volume of intake air badly which results a reduced volumetric efficiency. As blow by increases, during the combustion the engine power decreases because some of the high-pressure mixture will be lost which is pushing on the piston. When the expanding gases slip past the ring, they cannot as effectively push the piston down. As a result, the engine will have less power, which also results in a loss of fuel economy.

Blow by gases is a formation of the leak from the cylinder and other gases come from other parts in the engine. These gases join in the crankcase area which is the region above the oil sump. As a nature of this region, the blow by gases mix with the engine oil in here. In the old technology engines, this blow by gases were being released to the atmosphere that causes high oil consumption. With the improvement of new engine technologies, currently these blow by gases are being returned to the engine. In this case, the important thing is to separate the oil from the gas not to burn the oil in the cylinder and not to increase the oil consumption. Because of this, the oil must be separated from blow by gases through a crankcase ventilation system before joining the air intake system. Practically, it is not possible to separate the oil completely. The general effects of blow by are increase in oil consumption with a decrease in combustion efficiency due to uncontrolled gas content in the cylinder.

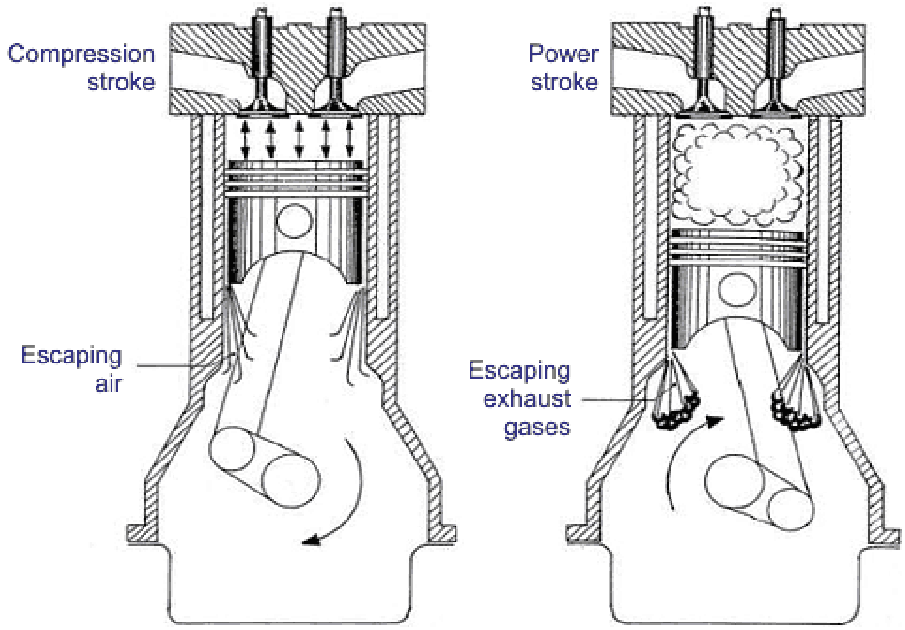

Figure 2.7 : Blow by – gas leakage through the piston rings [25].

3. THEORY AND MODEL

3.1 Piston Ring Pack Dynamics

One of the most important component in an internal combustion engine is the piston that transfers the force from the expanding gas in the cylinder to the crankshaft via a connecting rod. Piston feature includes the piston head, piston pin bore, piston pin, ring grooves and piston rings.

Piston head is the closest surface of the piston to the cylinder head that is subjected to the high combustion pressures and temperatures during the engine operation [26]. Piston head also includes the combustion chamber with a suitable geometrical form where the fuel and air mixture burns. This can be optimized with the CAE analysis to be able to provide a good quality combustion characteristics.

Piston pin is a cylindrical shaft that connects the small end of the connecting rod to the piston through a piston pin bore for the transfer of the force between the crankshaft and piston assembly.

Piston ring is a critical part of a power conversion system that controls many significant parameters for the engine performance and durability such as oil consumption, blow by and compression characteristics. The primary function is to seal off the combustion pressure between the piston and cylinder while it controls the oil and transfers the heat [19]. Most widely used piston rings include the compression ring, wiper ring and oil ring within the same given order.

A compression ring (also known as top ring, first compression ring) is located in the first groove of the piston that is the closest one to the head of the piston. With the pressure of combustion, gases flow through the ring groove and push the ring against the cylinder wall in order to provide a seal between the piston and cylinder liner.

A wiper ring (also known as scrapper ring, second compression ring) is located in the second groove with generally in tapered form to be able to wipe the cylinder wall from the excess oil for the lubrication of the piston skirt and first compression rings. Practically all of the scrapper rings used are the rings with a step recessed into the bottom outer face to assure an effective oil scrapping. Correct installation of these rings is another important criterion not to cause and excessive oil consumption by wiping the lubricating oil toward the combustion chamber. Beside this, a wiper ring can seal the leaked combustion gases that pass by the first compression ring.

An oil ring is located in the third ring groove that is closest to the crankcase area to wipe and return the excess oil from cylinder wall to the oil pan. It includes two running surfaces with a hole into the radial center of the ring to allow the flow off excess oil back to the oil reservoir. Compared to the two other rings described above, the oil ring has the highest inherent pressure [26].

3.2 Forces Acting on a Piston Ring

During the operation of the engine, the piston ring is subjected several forces as a result of movement of the piston, piston friction and combustion gas pressure. To explain the mathematical relationship for the stabilized flank contact and therewith the fundamentals of the piston ring position change, the model is simplified with below items:

a) A rectangular ring is used and approached as single masses.

b) The pressure function above and under the ring is linear.

c) In comparison to the gas pressure, friction forces are negligible.

d) The radial mass forces of the rings are neglected due to minor changes caused by oil film thickness [11].

The forces acting on a piston ring can be shown as in Figure 3.1.

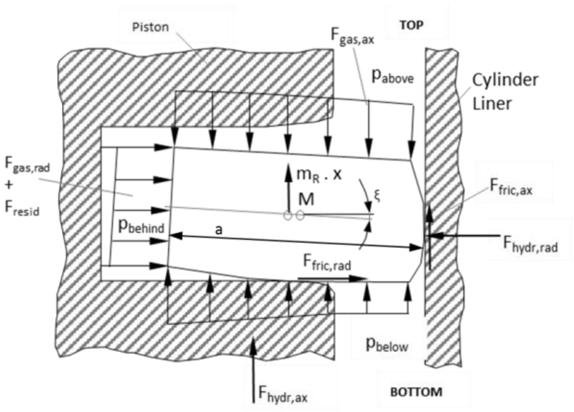

Figure 3.1 : Forces acting on a piston ring [15].

During the motion of the piston axially in downwards and radially to the left side, in the axial direction the forces acting on a ring are shown as below:

- Force caused by the mass of the ring, F_{mass}
- Force caused by the friction between liner and ring running surface, $F_{fric,ax}$
- Force caused by the gas pressure, $F_{gas,ax}$
- Damping force caused by oil filling of the groove, $F_{hydr,ax}$
- Bending force caused by interaction between thrust and anti-thrust side, F_{bend}

On the other side, in the radial direction the piston ring is subjected to below forces:

- Ring tension force, $F_{tension}$
- Force caused by the gas pressure, $F_{gas,rad}$
- Force caused by the friction between ring and ring groove, $F_{fric,rad}$
- Force caused by hydrodynamic pressure in the gap between cylinder liner and ring running surface, $F_{hydr,rad}$

The equilibrium of the contact forces define the ring motion in the axial direction. If it is accepted that the ring is in contact with the groove flank, the contact force can be calculated with equation 3.1:

$$F_{contact,ax} = F_{mass} + F_{fric,ax} + F_{gas,ax} + F_{bend} \tag{3.1}$$

The resulting axial gas forces can be described as a function of the pressure above and under the ring. Following equations will show that the resulting gas force is independent from the gas pressure behind the ring. The pressure in the top clearance of the ring groove can be formulated with below equation where the forces are positive in upward direction.

$$P_{top}(x) = -\frac{1}{2}\,(P_{above} + P_{behind}) - \frac{x}{a}\,(P_{above} - P_{behind}) \tag{3.2}$$

At the bottom clearance:

$$P_{bottom}(x) = \frac{1}{2}\,(P_{under} + P_{behind}) + \frac{x}{a}\,(P_{below} - P_{behind}) \qquad \textbf{(3.3)}$$

The resulting gas pressure, $P_r(x)$ is the sum of $P_{top}(x)$ and $P_{bottom}(x)$ where the pressure difference, ΔP is defined as $\Delta P = P_{above} - P_{under}$.

$$P_r(x) = -\frac{1}{2}\,\Delta P - \frac{x}{a}\,\Delta P \qquad \textbf{(3.4)}$$

The axial gas force and moment can be calculated as an integral of the resulting gas pressures acting on a ring with below equations. The resulting moment will be equal to gas moment because the mass force causes no moment at the center of the mass.

$$F_{gas,ax} = \int_{-\frac{a}{2}}^{\frac{a}{2}} P_r(x)\,dx$$

$$F_{gas,ax} = -\frac{1}{2}\,a\,\Delta P \qquad \textbf{(3.5)}$$

$$M_{gas,ax} = \int_{-\frac{a}{2}}^{\frac{a}{2}} F_{gas,ax}\,x\,dx$$

$$M_{gas,ax} = M_{contact,ax} = -\frac{1}{12}\,a^2\,\Delta P \qquad \textbf{(3.6)}$$

3.3 Inter Ring Pressure Calculation – Orifice and Volume Method

The piston assembly is the most complex tribological system in the internal combustion engine and must fill a number of important roles [20]. The piston ring’s primary objective is to provide a seal by preventing the combustion gases to escape the crankcase area from the combustion chamber during the engine operation. However, the piston rings also provide a passage way for the gases to escape past to their design structure and configurations. Minimizing the leakage rate from the piston rings is one of the most important challenge in the internal combustion engine technology as without an effective seal the gas pressure in the combustion chamber would be lower during the combustion and expansion and reducing the efficiency of the engine. In addition to this, gases escaping from the combustion chamber will come into contact with lubricating oil leading to degradation and reduced effectiveness of the oil.

The gas leaked from the groove flank top and bottom clearances, liner and ring running surface clearances and ring end gaps create gas pressure behind the ring in the groove and on the piston lands between the rings. The amount of gas pressure behind the ring defines the sealing forces while the gas pressure between the rings controls the oil consumption and blow by characteristics of an engine due to effects on the ring motion.

The piston rings are also required to control the flow of lubricant traveling from the sump through the ring pack and into the combustion chamber. This is a compromise between supplying enough oil to the piston assembly for effective operation while keeping the quantity reaches the combustion chamber to a minimum to limit harmful exhaust emissions.

To simplify the problem of analysis, a mathematical model is developed to study the lubrication between the rings and cylinder liner, and can determine the gas flow through the piston rings and the inter-ring gas pressures [20].

As stated earlier, the gas pressure behind the ring provides a major contribution to the sealing force. In the case of the top compression ring, the gas in the combustion chamber passes down the clearance space between the piston crown land and the cylinder liner and then into the top ring groove to load the rear face of the ring. There will be some differences in this pressure compared to the combustion pressure, however it is very usual in lubrication analyses of piston ring pack to assume that the pressure in the top ring groove is equal to the combustion chamber pressure at all times. Therefore, the first assumption for the prediction of the inter-ring pressures, the top ring groove and land pressure will be deemed same as with the combustion pressure.

Flow of gas into the volume formed between the piston rings and between the first and second ring is strictly limited by the top compression ring. If it is assumed that the lubricant occupies any clearance between the ring and cylinder liner and no gas passes between the ring and the flank of the ring groove, gas leakage will be restricted to an orifice formed by the ring gap and radial clearance between the ring and liner. The similarity between the mechanisms of gas flow through a ring pack and that through a labyrinth seal prompted Eweis (1935) to propose and “orifice and volume” method for calculation of inter-ring pressures. A more complete account of this approach has been presented by Ting and Mayer (1974).

The gas flow between the rings is assumed adiabatic and equation for the mass rate of flow through each orifice neglecting potential energy changes;

$$\frac{P_{m-1}}{\rho_{m-1}}+\frac{\mathrm{v}^2{}_{m-1}}{2}+u_{m-1}=\frac{P_m}{\rho_m}+\frac{\mathrm{v}^2{}_m}{2}+u_m=constant$$
$$\frac{p}{\rho}+u=h=c_pT \tag{3.7}$$

If v_m represents the mean velocity of the jet of the gas entering to volume (m) through the orifice and the kinetic energy of the fluid in the reservoir (m-1) is negligible.

$$\mathrm{v}_m=\sqrt{\frac{2k}{k-1}R\,T_{m-1}(1-\frac{T_m}{T_{m-1}})} \tag{3.8}$$

If the flow is assumed adiabatic, below thermodynamic transformation can be done and the velocity of the gas jet can be expressed as a function of the gas pressure.

$$\frac{T_m}{T_{m-1}}=(\frac{P_m}{P_{m-1}})^{\frac{k-1}{k}} \tag{3.9}$$

$$\mathrm{v}_m=\sqrt{\frac{2k}{k-1}R\,T_{m-1}(1-(\frac{P_m}{P_{m-1}})^{\frac{k-1}{k}})} \tag{3.10}$$

3.3.1 Calculation of the Ring End Gap Flow Rate

The general flow formula is a function of specific gravity, cross sectional area and velocity. With the addition of the discharge coefficient of orifice, time dependent flow rate from the ring end gap ($\dot{m}_a$) can be formulated with below first order differential equations [1].

$$\frac{dm_{a_{m-1}}}{dt} = K_C A_m \sqrt{\frac{2gk}{R(k-1)T_{m-1}}}\, p_{m-1} \left(\frac{p_m}{p_{m-1}}\right)^{\frac{1}{k}} \sqrt{1 - \left(\frac{p_m}{p_{m-1}}\right)^{\frac{k-1}{k}}}$$

$$\frac{dm_{a_m}}{dt} = K_C A_{m+1} \sqrt{\frac{2gk}{R(k-1)T_m}}\, p_m \left(\frac{p_{m+1}}{p_m}\right)^{\frac{1}{k}} \sqrt{1 - \left(\frac{p_{m+1}}{p_m}\right)^{\frac{k-1}{k}}} \qquad \textbf{(3.11)}$$

The studied ring pack as shown in Figure 3.2 consists two compression rings and one oil ring. If the gas seal effect due to oil ring is assumed negligible, the ring pack can be represented as a one-chamber passage system with P_i ,V_i,T_i indicating the combustion chamber pressure, volume and temperature.

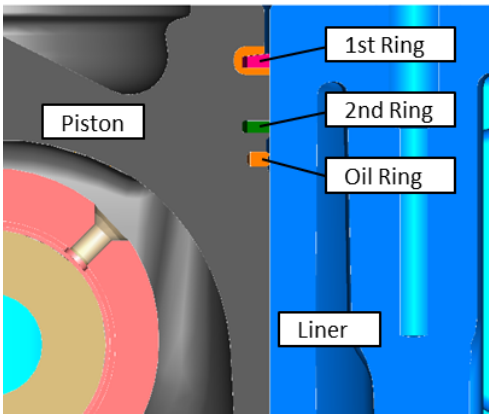

Figure 3.2 : Ring pack configuration of studied engine.

For a two ring – one chamber passage system, the ring end gap flow formulas can be expressed as a function of crank angle with below assumptions [1]:

$$P_m = \frac{p_m}{p_0}\ , \ \bar{m}_{a_m} = \frac{m_{a_m}}{m_0}\ , \ \bar{T}_m = \frac{T_m}{T_i}\ , \theta = wt,$$

$$K_i = \frac{K_C A_1}{V_2 w}\sqrt{\frac{2gkRT_i}{k-1}}\ , \qquad m_0 = \frac{V_2 p_0}{RT_i} \qquad \textbf{(3.12)}$$

When the critical pressure ratio ($P_C\,/P_m$) is reached, the flow discharge rate remains constant and equal to maximum value.

Critical pressure ratio is given by with 1,3 adiabatic exponent number [1];

$$\frac{P_C}{P_m} = \left(\frac{2}{k+1}\right)^{\frac{k}{k-1}} = 0{,}546 \qquad \textbf{(3.13)}$$

Flow discharge rate;

$$\left(\frac{P_C}{P_m}\right)^{\frac{1}{k}}\sqrt{1-\left(\frac{P_C}{P_m}\right)^{\frac{k-1}{k}}} = 0{,}227 \qquad \textbf{(3.14)}$$

First compression ring end gap flow [1];

$$\frac{d\bar{m}_{a_1}}{d\theta} = K_i\,\frac{P_1}{\sqrt{\bar{T}_1}}\left(\frac{P_2}{P_1}\right)^{\frac{1}{k}}\sqrt{1-\left(\frac{P_2}{P_1}\right)^{\frac{k-1}{k}}} \qquad ,\frac{P_2}{P_1} > 0{,}546$$

$$\frac{d\bar{m}_{a_1}}{d\theta} = K_i\,\frac{P_1}{\sqrt{\bar{T}_1}}0{,}227 \qquad ,\frac{P_2}{P_1} < 0{,}546 \qquad \textbf{(3.15)}$$

Second compression ring end gap flow [1];

$$\frac{d\bar{m}_{a_2}}{d\theta} = K_i\,\frac{A_2}{A_1}\frac{P_2}{\sqrt{\bar{T}_2}}\left(\frac{1}{P_2}\right)^{\frac{1}{k}}\sqrt{1-\left(\frac{1}{P_2}\right)^{\frac{k-1}{k}}} \qquad ,\frac{1}{P_2} > 0{,}546$$

$$\frac{d\bar{m}_{a_2}}{d\theta} = K_i\,\frac{A_2}{A_1}\frac{P_2}{\sqrt{\bar{T}_1}}0{,}227 \qquad ,\frac{1}{P_2} < 0{,}546 \qquad \textbf{(3.16)}$$

3.3.2 Calculation of the Ring/Liner and Ring/Groove Gas Flow Rate

In addition to Ting and Mayer (1974) model, Liu and Yongzhang (1986) took account the flow rates between the piston rings and cylinder liner and between the piston rings and groove during the analysis of sealing characterics of piston rings in a reciprocating compressor. These flow characteristics can be described as the flow in a thin clearance between two smooth surfaces. This problem can be solved in theory of two-dimensional uncompressible viscous laminar flow as Tian et al. showed that the gas flow through the channel between ring and groove has Reynolds number less than 2000 for even an extreme case where top ring flutters. Therefore, it is safe to assume that the gas flow between ring and groove is laminar [4] [13].

When the clearance between a ring and its groove is greater than the given oil film thickness, gas passes through the ring groove. Gas flow through ring/groove clearance occurs in two different situations:

- When a ring stabilized and sits on one side of its groove for long portion of a cycle, gas flows through the channel between the other side of the ring and its groove if the ring does not fully block the groove.
- When a ring is in transition, especially when a ring flutters, gas flows through the ring/groove clearance [3].

Following is the general expressions of the gas flow rates between the ring/liner and ring/groove that is derivated from Navier Stokes equations.

Flow rate between the rings/liner and rings/groove[4]:

$$\frac{dm_{b_m}}{dt} = \frac{\pi\ D\ \delta_a{}^3\ (p_m{}^2 - p_{m+1}{}^2)}{24\mu RT_m} \tag{3.17}$$

$$\frac{dm_{c_m}}{dt} = \frac{\pi D\delta_b{}^3 (P_m{}^2 - P_{m+1}{}^2)}{12\mu RT_m \ln(\frac{D}{D-2b})} \tag{3.18}$$

For two rings – one chamber passage system, the ring/liner and ring/groove flow formulas can be expressed as a function of crank angle with $\theta = wt$ transformation.

Flow Rate between first / second compression ring and liner:

$$\begin{aligned} \frac{d\bar{m}_{b_1}}{d\theta} &= \frac{\pi D\delta_{a_1}{}^3 \left(P_1{}^2 - P_2{}^2\right)}{24\ w\ \mu\ R\ T_1} \\ \frac{d\bar{m}_{b_2}}{d\theta} &= \frac{\pi D\delta_{a_2}{}^3 \left(P_2{}^2 - 1\right)}{24\ w\ \mu\ R\ T_2} \end{aligned} \tag{3.19}$$

Flow Rate between first / second compression ring and groove:

$$\begin{aligned} \frac{d\bar{m}_{c_1}}{d\theta} &= \frac{\pi D\delta_{b_1}{}^3 \left(P_1{}^2 - P_2{}^2\right)}{12\ w\ \mu\ R\ T_1 \ln(\frac{D}{D-2b})} \\ \frac{d\bar{m}_{c_2}}{d\theta} &= \frac{\pi D\delta_{b_2}{}^3 \left(P_2{}^2 - 1\right)}{12\ w\ \mu\ R\ T_2 \ln(\frac{D}{D-2b})} \end{aligned} \tag{3.20}$$

3.3.3 Calculation of the Second Land Pressure

For the calculation of the inter-ring pressures between the first and second compression rings, the gas is assumed to be ideal gas as shown in **(3.21)**. Following is the derivation of the second land pressure between the top ring and second ring, represented by this model.

$$p_m V_m = \left(m_0 + m_{in_{m-1}} + m_{out_m}\right) R T_m \tag{3.21}$$

By applying the ideal gas law equation for determination of the pressure between first and second ring, the basic pressure equation is reached in **(3.23)** by using the transformation in **(3.22).**

$$P_2 m_0 R T_1 = \left(\Sigma m_1 - \Sigma m_2\right) R T_1 \tag{3.22}$$

$$\frac{dP_2}{d\theta} = \overline{T}_1 \; x \left(\Sigma \frac{dm_{in_1}}{d\theta} - \Sigma \frac{dm_{out_1}}{d\theta}\right) \tag{3.23}$$

The total inlet and outlet flow rates through the second land are shown as below in **(3.24)**.

$$\begin{aligned} \Sigma \frac{dm_{in_1}}{d\theta} &= \frac{d\overline{m}_{a_1}}{d\theta} + \frac{d\overline{m}_{b_1}}{d\theta} + \frac{d\overline{m}_{c_1}}{d\theta} \\ \Sigma \frac{dm_{out_1}}{d\theta} &= \frac{d\overline{m}_{a_2}}{d\theta} + \frac{d\overline{m}_{b_2}}{d\theta} + \frac{d\overline{m}_{c_2}}{d\theta} \end{aligned} \tag{3.24}$$

To be able to reach the final pressure formula, derivation of **(3.15)**, **(3.16)**, **(3.19)** and **(3.20)** needs to be placed into the **(3.23)** by thinking the total mass flow rates in **(3.24)**. In here, two new variables, “C” & “E” have been defined in **(3.25)** to simplify the equation [4]. After then, crank angle dependent second land pressure can be formulated as in **(3.26)**.

$$C = \frac{\pi D}{24\, h} \;, \qquad E = \frac{\pi}{12 \ln\left(\frac{D}{D - 2b}\right)} \tag{3.25}$$

$$\begin{aligned} \frac{dP_2}{d\theta} = \overline{T}_i \Bigg(K_i \frac{P_1}{\sqrt{\overline{T}_1}} \left(\frac{P_2}{P_1}\right)^{\frac{1}{k}} \sqrt{1 - \left(\frac{P_2}{P_1}\right)^{\frac{k-1}{k}}} + \frac{\left(C\, \delta_{a_1}{}^3 + E\, \delta_{b_1}{}^3\right)\left(P_1{}^2 - P_2{}^2\right)}{w\, \mu\, R\, T_i} \\ - K_i \frac{A_2}{A_1} \frac{P_2}{\sqrt{\overline{T}_2}} \left(\frac{1}{P_2}\right)^{\frac{1}{k}} \sqrt{1 - \left(\frac{1}{P_2}\right)^{\frac{k-1}{k}}} - \frac{\left(C\, \delta_{a_2}{}^3 + E\, \delta_{b_2}{}^3\right) x \left(P_2{}^2 - 1\right)}{w\, \mu\, R\, T_2} \Bigg) \end{aligned} \tag{3.26}$$

3.4 Modelling the Gas Flows

As presented in Section 3.3, a mathematical method has been evaluated to calculate the inter ring volume pressure distributions for an engine cycle of 9.0L Heavy Duty Truck Diesel engine ring pack. The resulting pressure figures are one of the key parameters to define the ring pack characteristics of an engine. In addition, same pressure distribution are used for the determination of the oil film thickness with the pressure information behind the ring. In this section, the flow modelling method through the ring pack which is a key parameter during the calculation of inter ring pressures will be explained with the direction of the flow dependent on the adjacent chamber pressure conditions.

The studied engine’s piston has total 3 rings as first compression ring, second compression ring and an oil ring. Before starting to build the model, below assumptions have been made after investigation in the literature:

- The gases escape past the piston by a labyrinth passage way.
- The ring end gaps are the most important opened area for the gases to leak out and the volumes between the rings can be assumed as a passage system with series of chambers which represents the inter ring areas as in Figure 3.2.
- Depends on the piston ring’s position, cylinder / piston conformability or pressure balance at the inlet and outlet of the chambers, additional gas leakage from liner and ring grooves can be included.
- The chambers are connected to each other by a square edged orifices that represents the gaps for the gases to leak out.

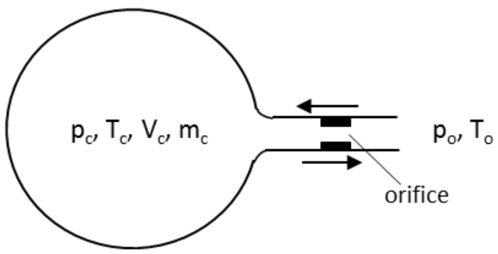

Figure 3.3 : Gas exchange through the chambers [15].

- Each inter ring chamber has basically two openings which allows gases to flow in or out.

- The gas flow is assumed to be unsteady adiabatic flow by ideal gas law.
- The gas flow through the ring gaps is considered as one dimensional flow through an orifice with a constant discharge coefficient. That has been taken as “0.65” which is suitable for square edged orifices.
- The seal effect of the oil ring is negligible, so the model of the ring pack can be represented as a “Two Ring – One Chamber” passage system.
- The pressure under the second ring is considered as equal to crankcase pressure which is assumed as 1 bar.
- The gas temperatures in the chamber are assumed to be uniform during the cycle and equal to piston land surface temperatures which is already obtained previously.
- Depends on the pressure boundary conditions, four possible gas flow direction is considered as shown in Figure 3.4.

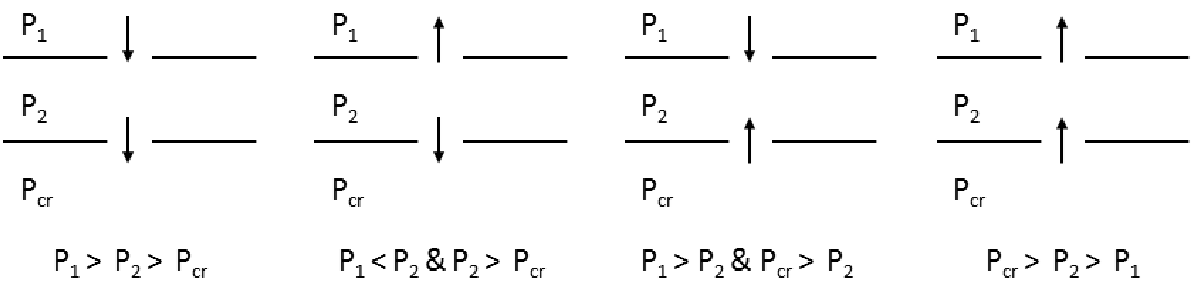

Figure 3.4 : Gas flow directions through the orifices.

- Engine running condition has been chosen as “1680 rpm full load” which a typical combustion pressure data was available experimentally from a dynamometer test engine.

With all above mentioned assumptions, the basic gas flow scheme has been created as in Figure 3.5 by thinking there is always a gas flow through the ring end gaps and microscopic flows through the ring running surface and ring grooves. Due to maximum velocity of the flow is limited to the sound velocity after a critical pressure ratio is reached, the ring end gap flow discharge rate has been considered as constant and equal to maximum value. Therefore, two boundary conditions have been defined for the determination of the end gap flow rate depends on critical pressure ratio.

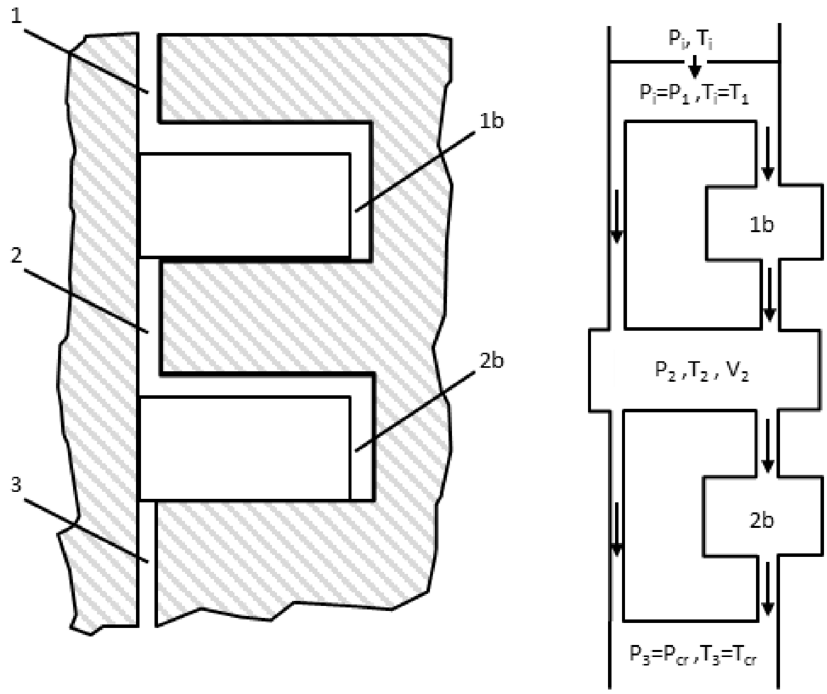

Figure 3.5 : Gas Flow Scheme – Modeled Labyrinth Passage Way

For the determination of the flow direction, two additional boundary conditions have been implemented according to combustion pressure and second land pressure. Although the ring sits on the downside or upside of the ring groove depending on the pressure variance between combustion and inter ring pressure, there is generally a microscopic flow area practically to the inter ring space through the ring grooves or liner. In the developed model, when the combustion pressure is higher than the second land pressure, it was considered that the first compression ring has a natural negative twist which made the gas flow through the liner or ring groove possible to the second land area. On the other hand, if the second land pressure gets higher than combustion pressure - especially in the expansion stroke, the first compression ring was assumed to have a positive twist intendancy which blocks the gas flow through the ring groove because of the contact points on the upside and downside.

By all this mentioned methodology and previously obtained gas flow and pressure equation in Section 3.3, a computer code has been evaluated which will be explained in Section 4 more detailed.

3.5 Friction Analysis

The second land pressure is one of the parameters that used for the calculation of frictional forces between the running surface of a ring and cylinder liner. After modelling the gas flows and calculating the second land pressures in the MATLAB code, the obtained results will be placed in another MATLAB code which has been established by Akalin and Newaz (2001) to simulate the lubrication and friction behaviour of the first compression ring of a highly loaded diesel engine for the determination of friction force, oil film thickness and power losses depending on the second land pressure magnitude. It uses the combustion pressure and the pressure between first and second compression rings as an input. This numerical method has been developed by Akalin and Newaz to predict frictional performance of piston ring and cylinder bore contact operating in the mixed lubrication regime, considering lubricant rupture location, surface flow factors, and metal-to-metal contact load. Asperity contact load has been included in the model due to its vital importance for the friction prediction and direct correlation has been identified between wear profile of cylinder bore and the load carried by surface asperities. For modelling the piston ring and cylinder bore contact, statistical surface asperity approach and Reynolds equation including surface roughness and flow factors have been used [22].

The assumptions for the model are as below:

- A fully flooded inlet boundary condition and Reynolds Boundary conditions for cavitation outlet zone are assumed.

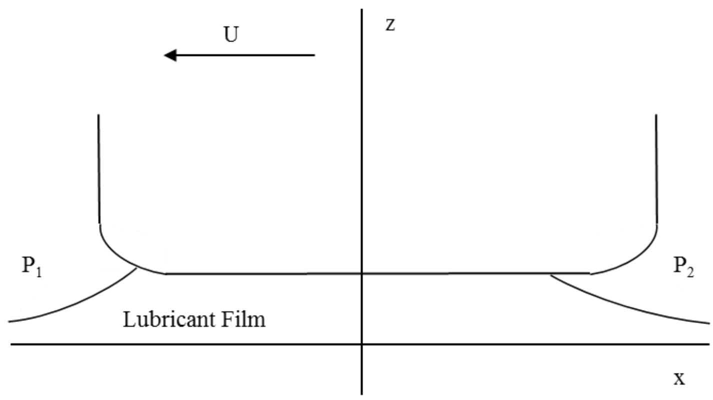

Figure 3.6 : Piston ring boundary conditions

- The pressure is equal to the gas pressure at the inlet of the lubrication region and sufficient lubricant is present at the leading edge of the ring.

- Reynolds (Swift-Stieber) boundary conditions are used for outlet boundary conditions where cavitation is present.

- Pressure gradient at the cavitation boundary is zero and the pressure is equal to the gas pressure at the outlet of lubricant region.

- Patir and Cheng's modified Reynolds equation, including surface roughness and surface flow factors and Grenwood and Tripp's statistical surface asperity approach has been used to model the piston ring and cylinder bore contact.

4. RESULTS AND DISCUSSION

As mentioned in Section 3, to be able to compute the second land pressures and gas flows through the ring pack, a mathematical code has been written in MATLAB program. Previously obtained the first order differential equations have been solved by iterations with the Euler Method by giving an initial value for second land pressure which was assumed to be equal to cylinder pressure at the start of intake stroke at -360°CA. The step size has been defined as 0.1 °CA and the experimentally available cylinder pressure data has been interpolated according to that. After the first iteration that was completed between -360 °CA and 360 °CA for one stroke, the pressure difference between the start and end of stroke points have been controlled as the gas pressures at that points need to be very close to each other theoretically to be able to have the accurate results from the model. According to this phenomena, the iterations continued until the pressure difference was less than a specified small convergence factor at specified points. In this model, the convergence factor has been defined as the first moment where the difference is lower than 0.001 arbitrarily. After the first results, the model has been tuned with specific items like blow by parameter, discharge coefficient.

The code starts the calculations with determination of the gas flow figures respect to crank angle over an engine cycle with the required pressure boundary conditions between top land and second land. After the calculation of the flow figures, by assuming and applying the ideal gas laws for an unsteady adiabatic flow, the pressure values have been calculated for the start of the engine cycle and iterated until the end of the stroke.

The model has been verified with the AVL Glide results which has been obtained by Gül (1997) for the same engine previously which has been used for oil consumption simulation study [21]. The results showed very good correlation especially in the region where the peak pressures were achieved during the compression and combustion stroke. After the verification, the effect of some of the important piston ring design parameter changes on the second land pressure had been investigated.

According to the information gathered in this step, a DoE Test Matrix have been created by a statistical engineering method to reach an optimized ring pack design. These will be shown in the next section in detailed.

4.1 Inputs

The program consists of constant and variable inputs. The constant inputs are mostly geometrical dimensions of piston, piston rings and cylinder. Additionally, some thermodynamic figures have been accepted as constant according to the assumptions made in section 3.4. The variables are the cylinder pressure data against to crank angle and viscosity of the gas dependent on gas temperature.

4.1.1 Constants

The values for the constants are shown below. All lengths are entered in meters, areas are in meters square, volume meters cubic and temperatures are in Kelvin.

- h1, h2 (1^{st} and 2^{nd} ring thickness): 3×10^{-3} m, 2.5×10^{-3} m
- w1, w2 (1^{st} and 2^{nd} ring end gap width): 0.375×10^{-3} m, 0.925×10^{-3} m
- A1, A2 (1^{st} and 2^{nd} end gap area): calculated from effective thickness and width of end gaps
- D (cylinder bore diameter): 115×10^{-3} m
- D_2ndland (piston 2^{nd} land diameter): 114.52×10^{-3} m
- h_2ndland (piston 2^{nd} land height): 11×10^{-3} m
- V1 (volume of inter ring space): calculated from D, D_2ndland and h_2ndland
- g (gravitational constant): 9.81 m/s^2
- k (isentropic exponent): 1.3 [1]
- R (ideal gas constant): 287 J/kgK
- ti (1^{st} groove gas temperature): 700 K [23]
- t1 (gas temperature in second land): 580 K [23]

Figure 4.1 shows the regions on the piston, rings and cylinder liner where the geometrical dimensions have been obtained. Figure 4.2 shows the temperature analysis of the piston.

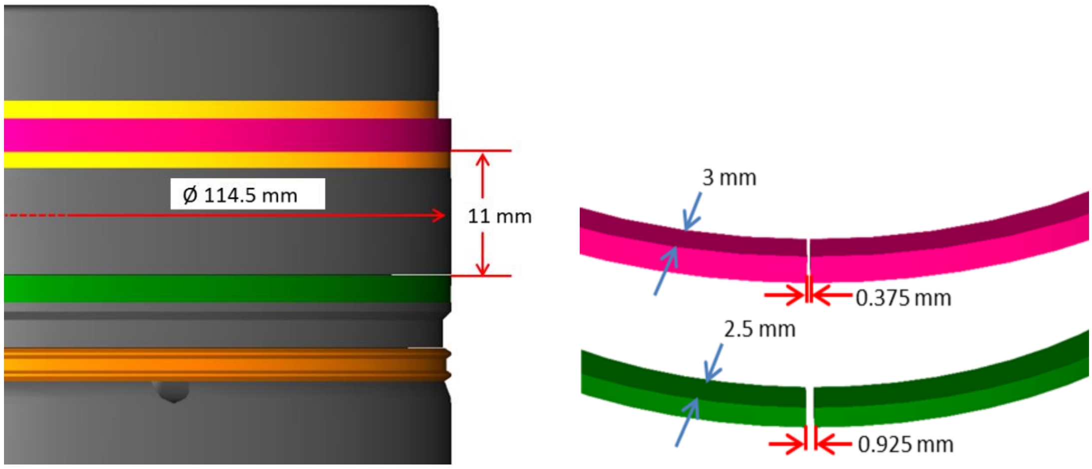

Figure 4.1 : Geometrical dimensions of piston, ring and liner.

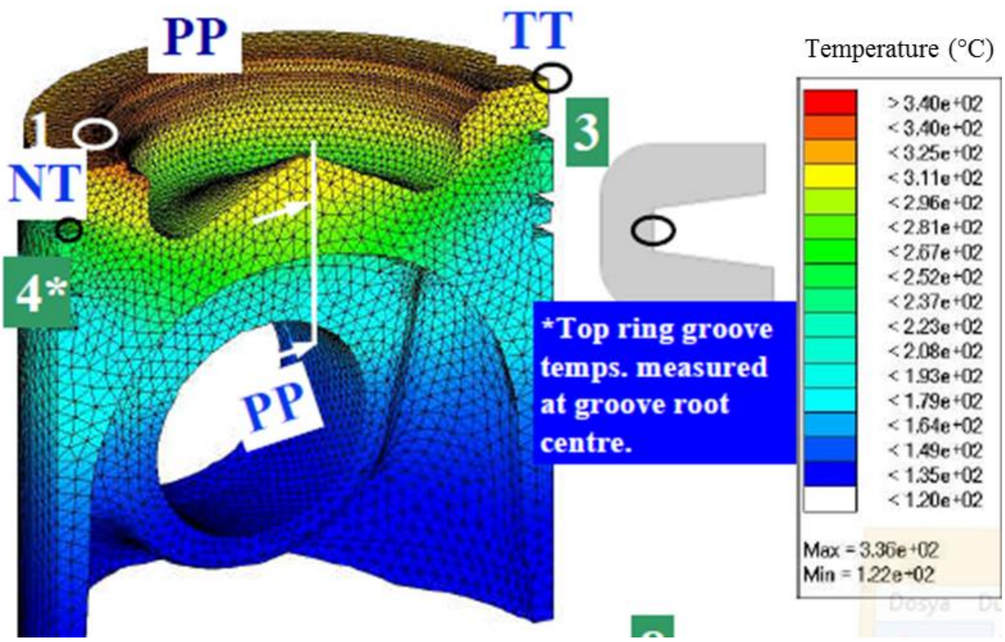

Figure 4.2 : Temperature analysis of the piston [23].

For the calculation in this section, the following assumptions were made:

- -360 °CA and 360 °CA region has been taken into account for a complete engine cycle.
- All of the dimensions were obtained from 2D technical drawings of the piston, piston rings and cylinder block.

- Due to available tolerances in the drawing, the average value has been taken for the specified engine components.
- There was no available crankcase pressure data so that it was assumed as equal to atmospheric pressure.
- Piston secondary motion has been neglected.

4.1.2 Variables

Two variable input has been entered into the program which one of them is the cylinder pressure, the other one is the viscosity. The cylinder pressure data as shown in Figure 4.3 have been obtained from a test engine on the dynamometer experimentally for 1680 rpm WOT condition. The second variable is the gas temperature dependent gas viscosity between the ring and groove which has been defined by Tian et al (1997).

The second input to the program is cylinder pressure curve, as shown in Figure 4.3.

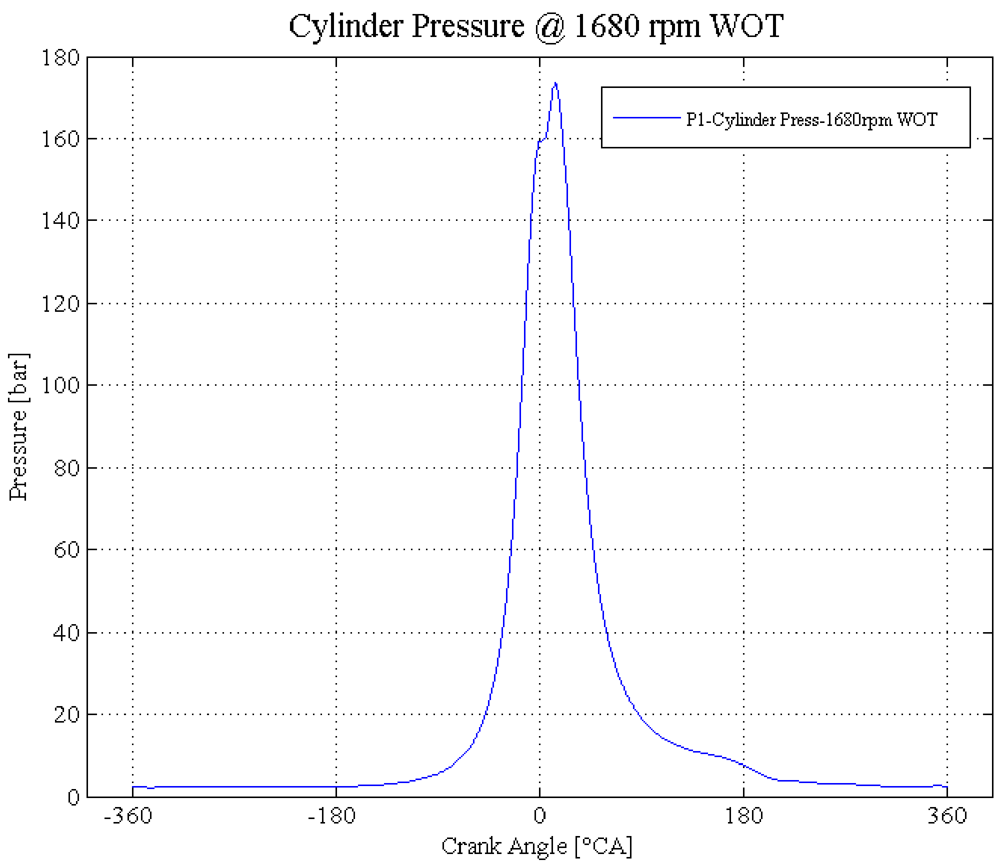

Figure 4.3 : Cylinder pressure curve used for this study.

4.2 Results

Using the flow dependent pressure formulas and experimentally obtained cylinder pressure data at 1680 rpm WOT, the second land pressure has been calculated and plotted as shown in Figure 4.4.

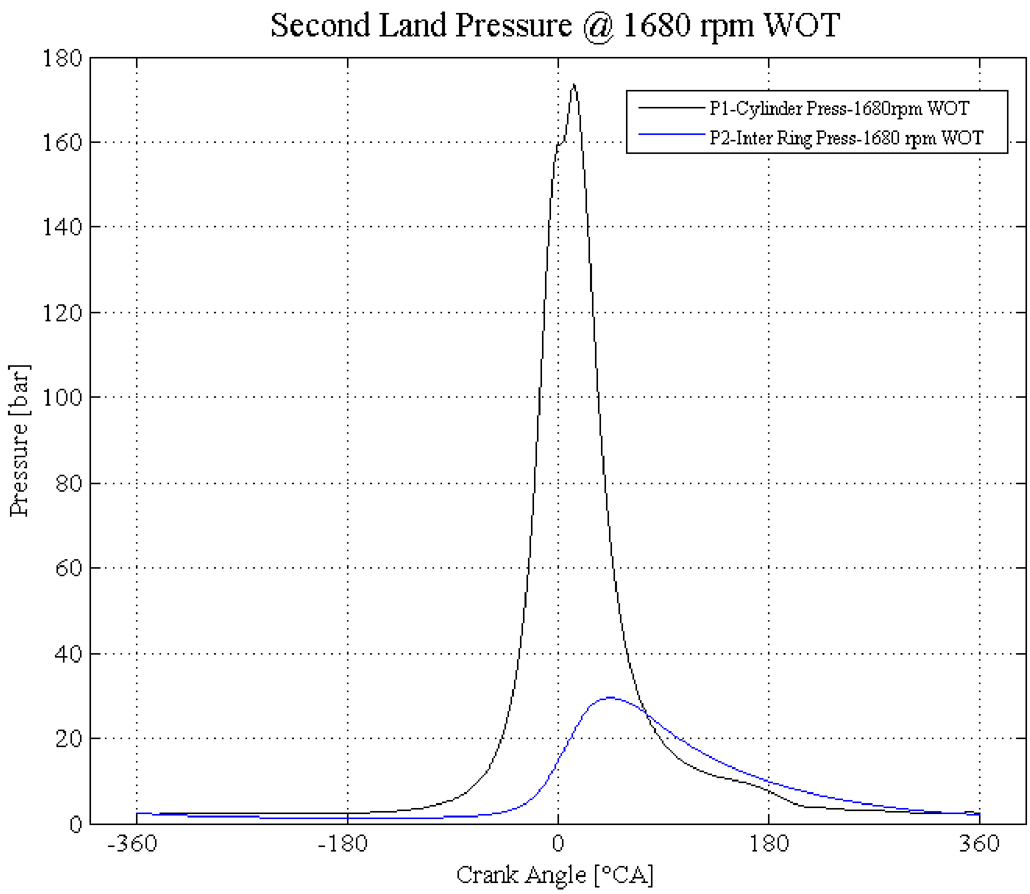

Figure 4.4 : Obtained second land pressure from MATLAB code.

As it can be seen from the Figure 4.4, during the intake stroke with the inertia of the piston and its related motion, the inter ring pressures are very close to the cylinder pressures which has low figures in that stage. With the starting of the compression stroke, even though there is a delay in the response, the inter ring pressures are started to increase with the increasing of the cylinder pressures. The maximum value of the pressure between 1st and 2nd ring is much lower than the cylinder pressure in the combustion chamber. Additionally, the combustion is started 14 °CA after TDC whereas the peak value of inter ring pressure is being reached at 45 °CA after TDC. This clearly indicates that there is a delay in the inter ring pressure response due to the fact that the orifice which represents the passage ways through the ring pack creates a restriction which lowers the pressure intensity and delays the pressure response in the following chamber.

During the late combustion and exhaust stroke, the cylinder pressures are decreased rapidly as no more fuel is being sent to the cylinder and with the expansion of the combustion gases, the pressure value gets smaller with the increasing of the gas volume. As it mentioned before, due to a delay in the inter ring pressure response, in this stages, the pressure between two rings can be greater than the cylinder pressure for a particular stage of crank angles. In this region, it is very possible that a reversed gas flow through the ring pack can occur.

After the evaluation of the data from the MATLAB code, the results have been compared as shown in Figure 4.5 with the results obtained from AVL Glide program by Gül (1997) during another study for the same engine.

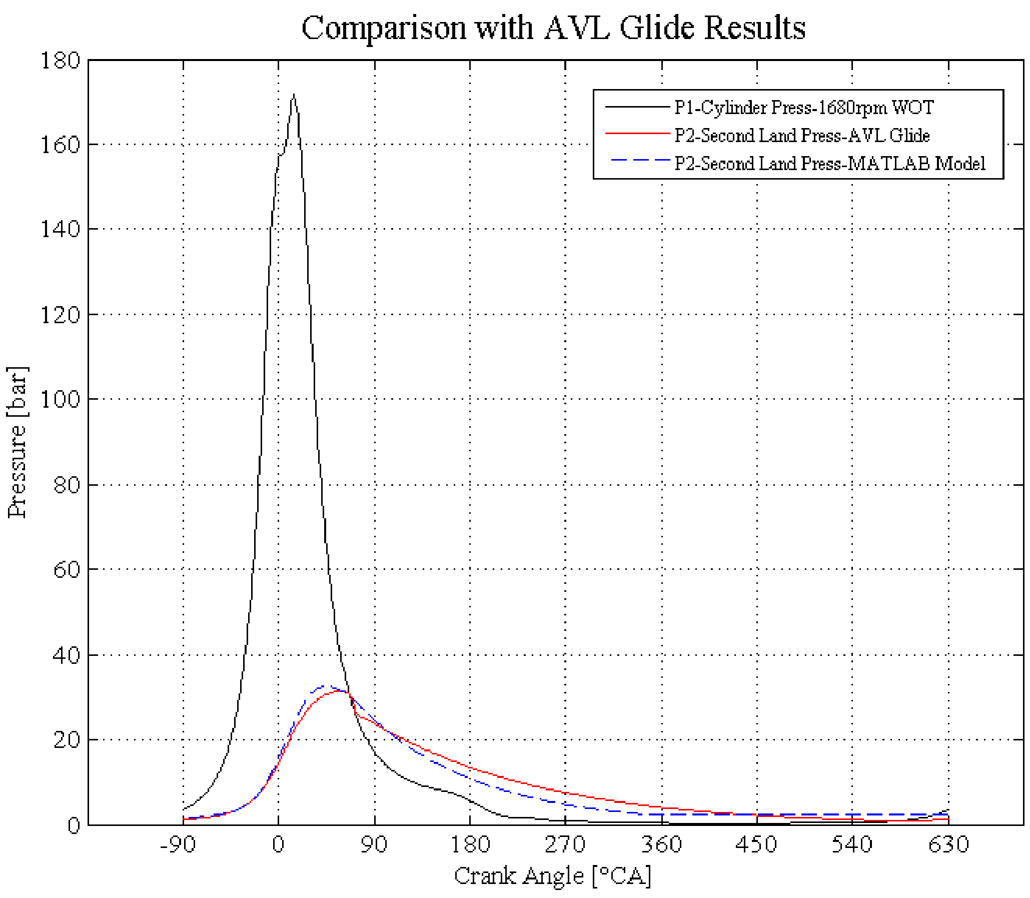

Figure 4.5 : Comparison of the results with AVL Glide.

The results obtained from the mathematical MATLAB code have shown a good agreement with the AVL Glide computed results which indicates that the model is good. The pressure trend is very close to each other during the compression and combustion stroke. The peak value of second land pressure has been predicted well with the code written in MATLAB. The pressure trend during the intake stroke is very close to each other and combustion pressure as expected. Only a difference was observed between two models during the expansion stroke where the second land pressure is higher than the combustion pressure. It is very possible to have a reverse flow and ring collapse in this stage. Since the MATLAB model neglect the movement of the ring, there is only a slight difference between MATLAB model and AVL Glide model during this stage.

In the literature, inter ring pressure related studies show that the piston ring characteristics are highly relevant for the engine performance, durability and reliability as the contribution of the inter ring pressures to the piston ring friction and thus to the engine efficiency. In order to design a robust and reliable ring pack, defining the optimal design parameters are very essential. To be able to assess the influence of the ring pack characteristics, in the following sections, the effect of the ring pack design parameters on the inter ring pressures will be studied in detail as this will provide a strong knowledge during the design of any piston ring pack in the future. The specifically studied parameters are as shown in Table 4.1

Table 4.1 : Piston/Ring design parameter list

Parameter	**Min Value**	**Nominal Value**	**Max Value**
[-]	**mm**	**mm**	**mm**
First Ring End Gap Width	0.300	0.375	0.450
Second Ring End Gap Width	0.800	0.925	1.050
Piston Second Land Height	9	11	13
Ring Discharge Coefficient [16]	0.60	0.70	0.83
First Ring Thickness	2.50	3.00	3.50
Second Ring Thickness	2.00	2.50	3.00

4.2.1 Effect of the First Compression Ring Gap Width

By changing the related geometrical dimensions in the MATLAB code, the inter ring pressures are simulated and plotted as shown in Figure 4.6. The simulation results show that the pressure in the second land is directly proportional with first end gap width as the flow rate will increase if a larger gap is chosen which will result the gas flow to be increased and the pressure as well.

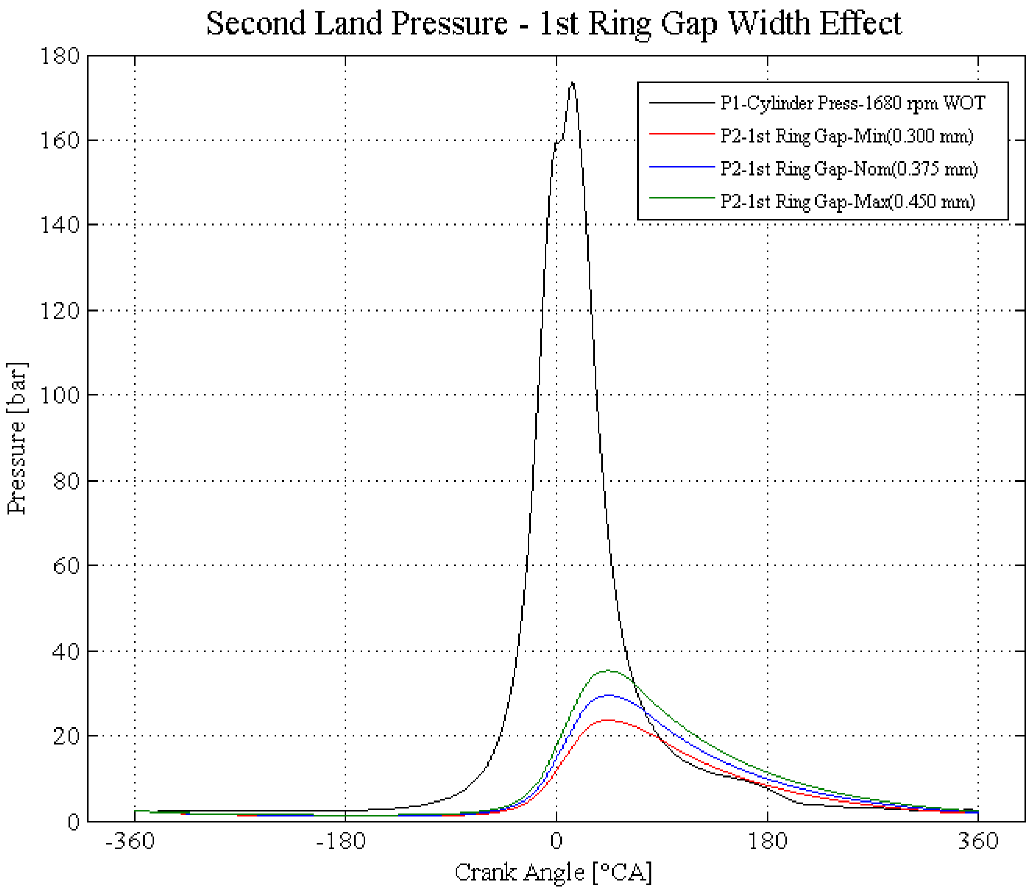

Figure 4.6 : First ring end gap width effect on second land pressures.

According to the comparison results, there is an increase about %50 on the inter ring pressure peaks between minimum and maximum first ring end gaps. Additionally, the maximum ring end gap results indicate a faster pressure drop in the expansion stroke due to higher pressure rate than cylinder and increased flow rate leaving the chamber in a reverse flow.

4.2.2 Effect of the Second Compression Ring Gap Width

By changing the related geometrical dimensions in the MATLAB code, the inter ring pressures are simulated and plotted as shown in Figure 4.7. That graph shows the effect of the second ring end gap width change on the inter ring pressures. Differently from the first ring end gap effect, it is clearly shown that the second ring end gap has a reverse effect on the second land pressure as expectedly. With the increasing of the second ring end gap width, the gas flow rate from the second land to third land will increase which will result a decreased pressure between the first and second ring. Although there is a pressure decrease with the increase of the end gap width, this is not a significant impact like the first ring end gap width.

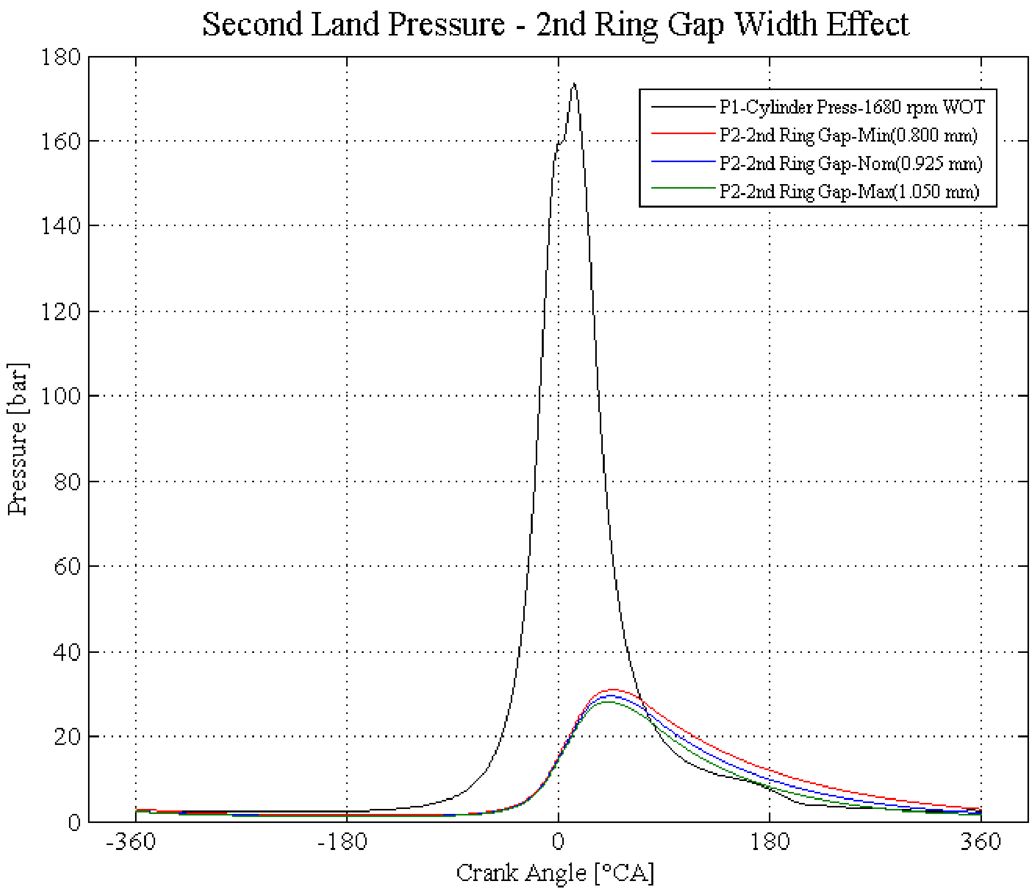

Figure 4.7 : Second ring end gap width effect on second land pressures.

4.2.3 Effect of the Second Land Height

To be able to simulate the inter ring space volume change, piston second land height has been modified in the MATLAB code, the inter ring pressures are calculated and plotted as shown in Figure 4.8.

By changing of the piston second land height, similar but more effective impact has been observed on the inter ring pressures with the second ring gap width increase. Increasing the second land height of the piston will result a decreased inter ring pressure in the increased volume between the first and second compression rings which is expected to see due to ideal gas law as the particle number in the gas will decrease.

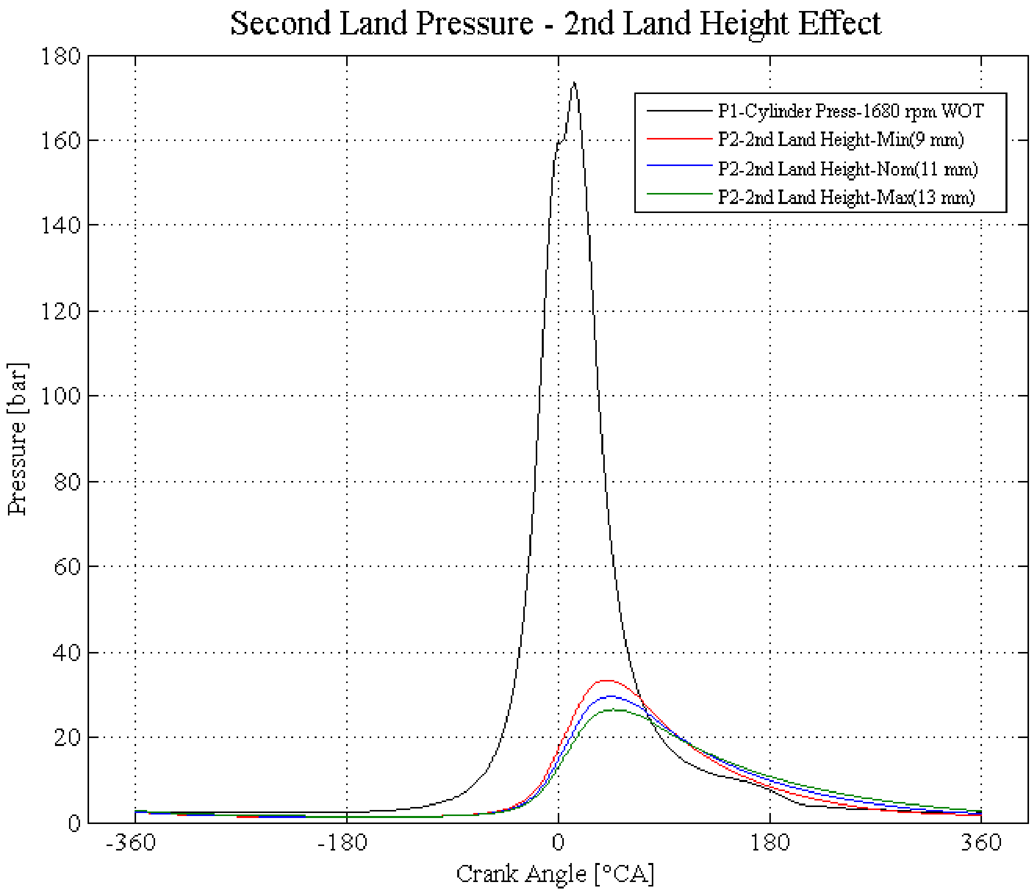

Figure 4.8 : Second land height effect on second land pressures.

4.2.4 Effect of the Ring Discharge Coefficient

Ring discharge coefficient is a specific parameter which defines the transition of the gas flow characteristics. By changing the related parameter K_c in the MATLAB code, the inter ring pressures are calculated again for 3 different K_c and plotted as shown in Figure 4.9.

The discharge coefficient of an orifice depends on its shape and upstream and downstream coefficients. In the literature, the discharge coefficient has been selected from 0.6 to 0.83. In this section, it is seen that the ring discharge coefficient has a direct influence on the inter ring pressures. The maximum second land pressure peak has been obtained with 0.83 naturally as the gas flow to second land has increased with this option. In open literature, it is noted that generally the value is selected as to be best fit with the experiments [16].

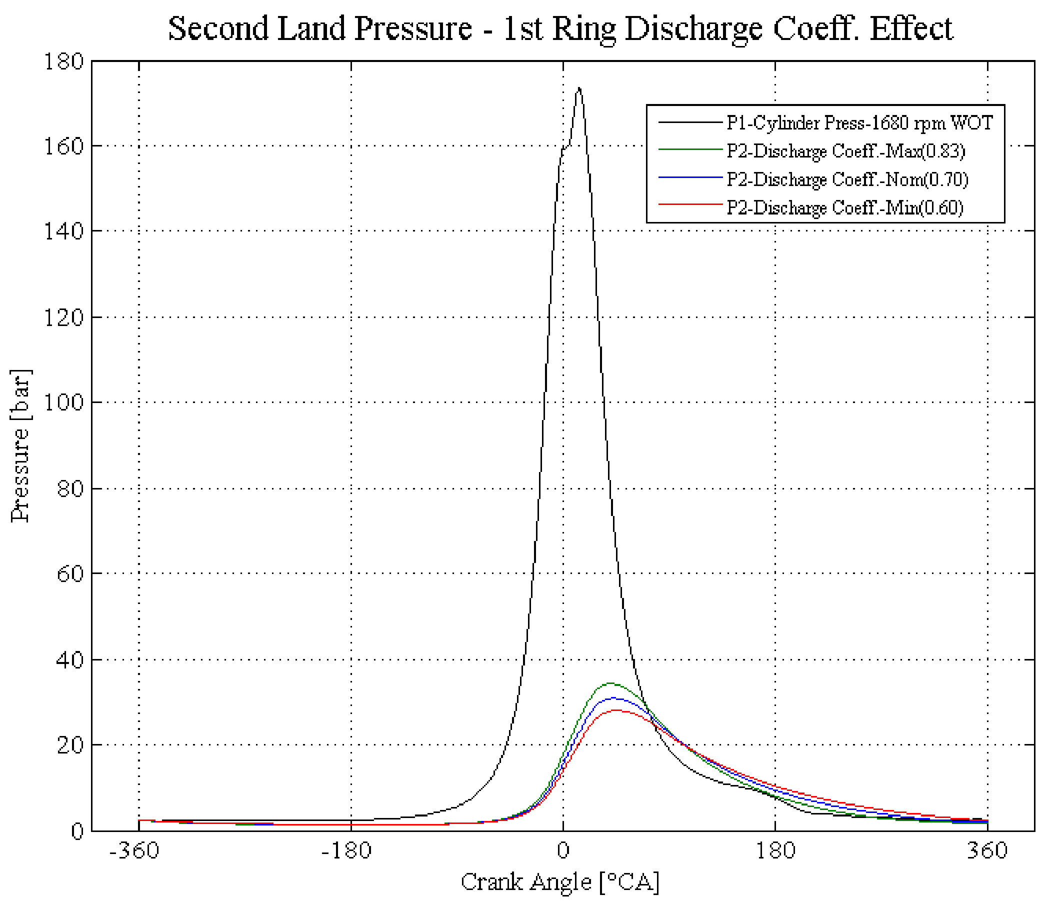

Figure 4.9 : Discharge coefficient effect on second land pressures.

4.2.5 Effect of the First Compression Ring Thickness

By changing the related geometrical dimensions in the MATLAB code, the inter ring pressures are simulated again and plotted as shown in Figure 4.10.

To be able to see the effect of the ring thickness on the second land pressure, three different thickness ring has been modelled and simulations have been run according to that. Generally 10% of total ring thickness stays outside of the ring groove. That effective length has been increased in that analysis in case of seeing the effect of any ring movement in backwards or forwards.

It is clearly seen that the second land pressure peaks have increased with a greater effective thickness as the cross sectional flow area of the first ring end gap gets larger and the gas flow into the volume between two rings are higher. This provides a similar effect with the increasing of the first ring end gap due to contribution to the cross sectional flow area.

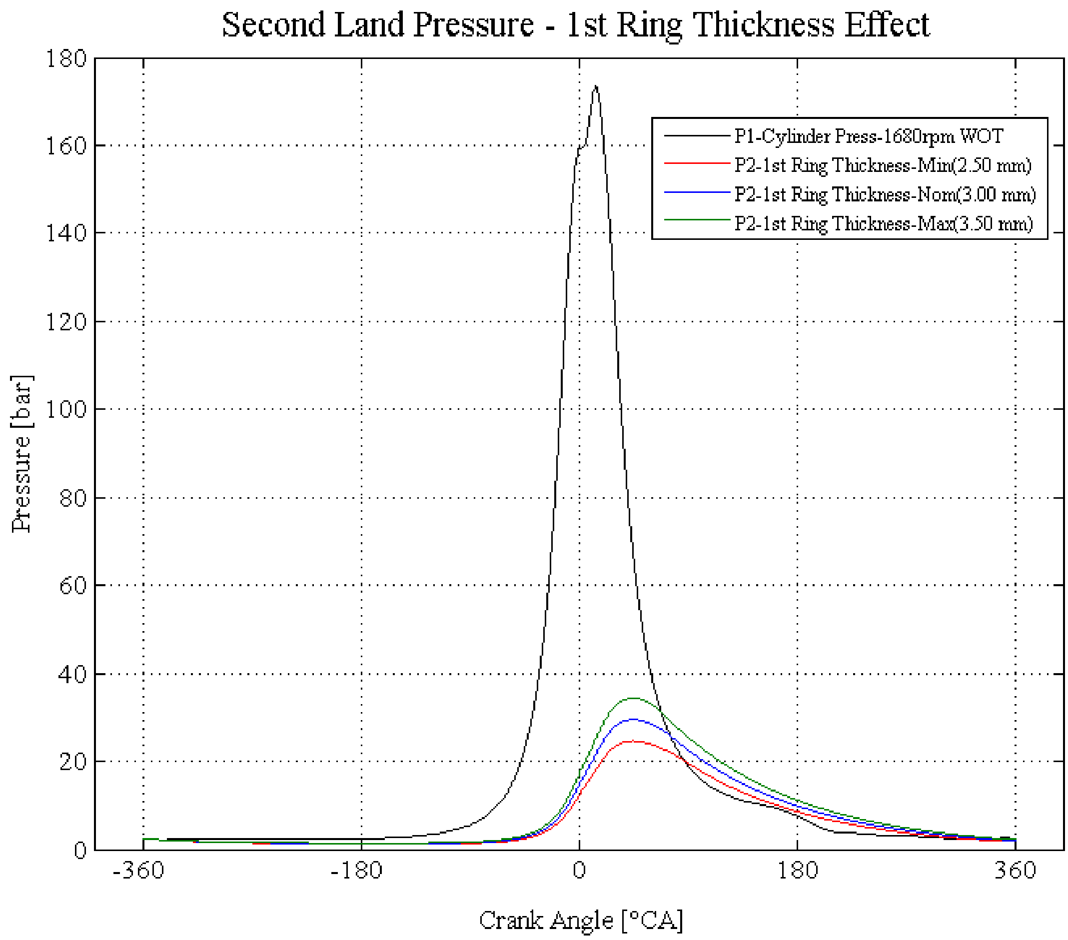

Figure 4.10 : First ring thickness effect on second land pressures.

4.2.6 Effect of the Second Compression Ring Thickness

By changing the related geometrical dimension “h2” in the MATLAB code, the inter ring pressures are calculated again and plotted as shown in Figure 4.11.

After the simulations with three different thickness of second compression ring, a similar effect has been observed on the second land pressures with the change of second ring end gap width. With the increasing of the second ring height, the cross sectional flow area of the second ring gets larger and the flow from second land to third land gets increased. As a result of this, outlet flow will increase while the second land pressure will decrease although it has not a major effect as the first ring thickness change.

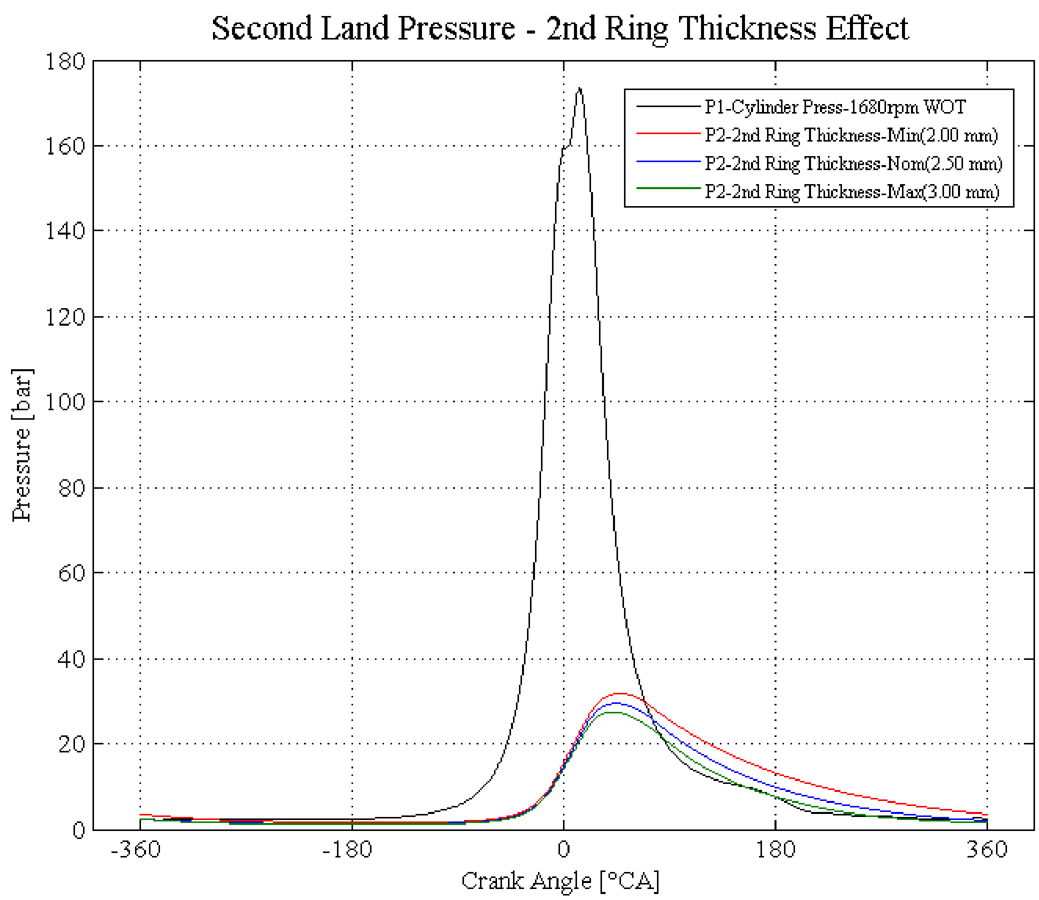

Figure 4.11 : Second ring thickness effect on second land pressures.

4.2.7 Effect of the First Ring / Liner Clearance

By changing the related geometrical dimension "sigmai" in the MATLAB code, the inter ring pressures are simulated and plotted as shown in Figure 4.12.

In the allowed design rules of a piston ring pack, two different ring/liner clearance have been chosen by considering the minimum and maximum oil film. As expected to be seen, the second land pressure peaks are higher with the larger first ring/liner clearance as the gas flow into the inter ring space volume gets higher.

In a normal operating conditions, it is not expected to see an important gas flow between the piston ring and cylinder block due to availability of lubricant film in that area. This analysis has been done to forecast some extreme conditions that can be faced during the life of an engine.

This phenomenon gives an idea what will be the result of losing the lubricant film between ring/liner, distorted cylinder bore or worn ring face.

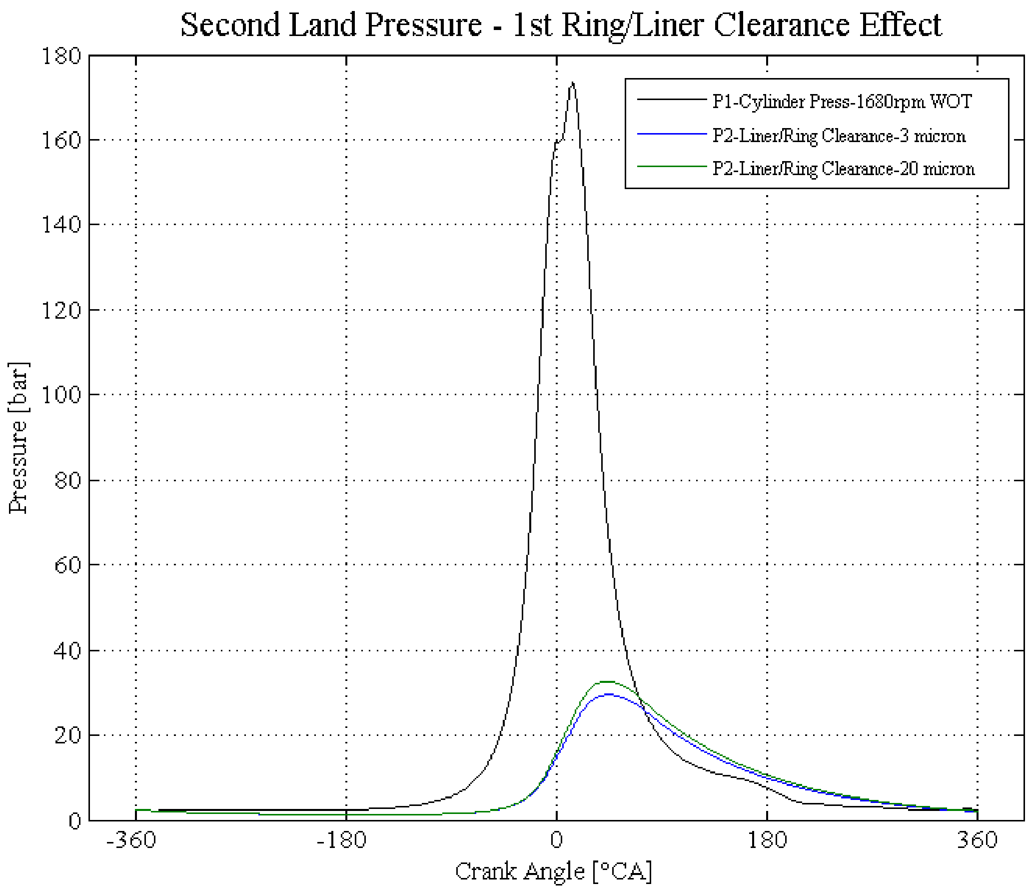

Figure 4.12 : First ring/liner clearance effect on second land pressures.

4.3 Sensitivity Analysis of Inter Ring Pressure with Ring Pack Configurations

As shown in Section 4.2, the influence of the piston ring pack behaviours on the inter ring pressures have been investigated individually. This analysis show that the piston ring design parameters have a considerable effect on the second land pressures by effecting the gas flow into the inter ring space.

In this section, by conducting a sensitivity analysis, the effect of the ring design parameters will be investigated by changing them in the same in minimum or maximum way. By contribution of different configurations, average effect of each parameter will be found separately. For this purpose, it is going to be taken advantage of statistical engineering methods which is called “Taguchi Method”.

Taguchi Method, also called the Robust Design method, greatly improves the engineering productivity by considering the environmental, manufacturing and component deterioration related noise factors. This method involves reducing the variation in a process through robust design of experiments to investigate how different parameters affect the mean and variance of a process performance characteristics. The experimental design proposed by Taguchi involves using orthogonal arrays to organize the parameters affecting process and the levels at which they should be varied. Instead of having to test all possible combinations, the Taguchi method tests pairs of combinations. This allows for the collection of the necessary data to determine which factors most affect product quality with a minimum amount of experimentation, thus saving time and resources [27].

The design parameters affecting the second land pressures have been determined in the Section 4.2 as it also can be seen in Table 4.3. The number of levels that the parameters should be varied at have been chosen as “minimum” and “maximum” value which has been represented as “-“ and “+” in the orthogonal array. In conclusion, 7 different parameters and 2 levels have been defined for the design of experiment studies and according to Table 4.2, L8 orthogonal array has been found as a suitable DoE matrix.

Table 4.2 : Orthogonal Array Selection

		Number of Parameters								
		2	**3**	**4**	**5**	**6**	**7**	**8**	**9**	**10**
Number of Levels	**2**	L4	L4	L8	L8	L8	***L8***	L12	L12	L12
	3	L9	L9	L9	L18	L18	L18	L18	L27	L27
	4	L16	L16	L16	L16	L32	L32	L32	L32	L32
	5	L25	L25	L25	L25	L25	L50	L50	L50	L50

After selection of the suitable orthogonal array, the MATLAB code has been run for eight different ring pack configuration and the results have been included into the table. With the help of this test matrix, it is possible to see the single effect of each parameter by changing the levels of all the other factors. As it can be seen in the Table 4.3, the resulting second land pressures vary between 22.45 and 60.31 bar in different conditions. This table will provide us the absolute effect information of each parameter separately which will be discussed in the following sections.

Table 4.3 : L8 Array DoE test matrix – Ring pack configurations

Row no.	1st Ring Gap Width [mm]	2nd Ring Gap Width [mm]	2nd Land Height [mm]	Discharge Coefficient [-]	1st Ring Thick. [mm]	2nd Ring Thick. [mm]	1st Ring/Liner Clearance [mm]	Second Land Pressure [bar]
1	-	-	+	-	+	+	-	22,45
2	+	-	-	-	-	+	+	34,09
3	-	+	-	-	+	-	+	32,59
4	+	+	+	-	-	-	-	24,81
5	-	-	+	+	-	-	+	26,77
6	+	-	-	+	+	-	-	60,31
7	-	+	-	+	-	+	-	21,81
8	+	+	+	+	+	+	+	39,71
							Average	**32,82**

In Experiment 1, it resulted with one of the lowest second land pressure peaks as in this configuration the first ring design parameters and the discharge coefficient which are most effective on the amount of leaked gases into the second land were chosen as in the minimum specification. So that the gas flow rate has decreased in a parallel way with the inter ring pressures.

In Experiment 4 and 7, it resulted with lower second land pressures again, even though not all of the first ring parameters are in minimum specification, some of the second ring design parameters (second land height, second ring thickness or second ring end gap width) are in maximum specification that increase the outlet flow rate from the second land with a pressure decrease which was previously mentioned in Section 4.2.2, 4.2.3 and 4.2.6.

In experiment 8, all of the first ring and second ring design parameters have been given as in maximum specification and that resulted with the second highest pressure values. By increasing all of the parameters in the same time, the factors have been balanced from each other naturally.

In Experiment 6, as it can be seen in the Table 4.3, the maximum pressure peaks have been reached as in this configuration the first ring parameters and the discharge coefficient are in maximum specification while the second ring's parameters are in minimum. By considering the results in Section 4.2, the gas flow rate has increased through the first ring but in the same time by giving the minimum values to the second ring, the gas flow rate has decreased through the second ring to the third land. Because of all these reasons, the flow difference gets higher which will result with the greatest pressure values in the second land.

The pressure figures for all of this configuration have been calculated in MATLAB code by changing the related design parameters and plotted as shown in Figure 4.13.

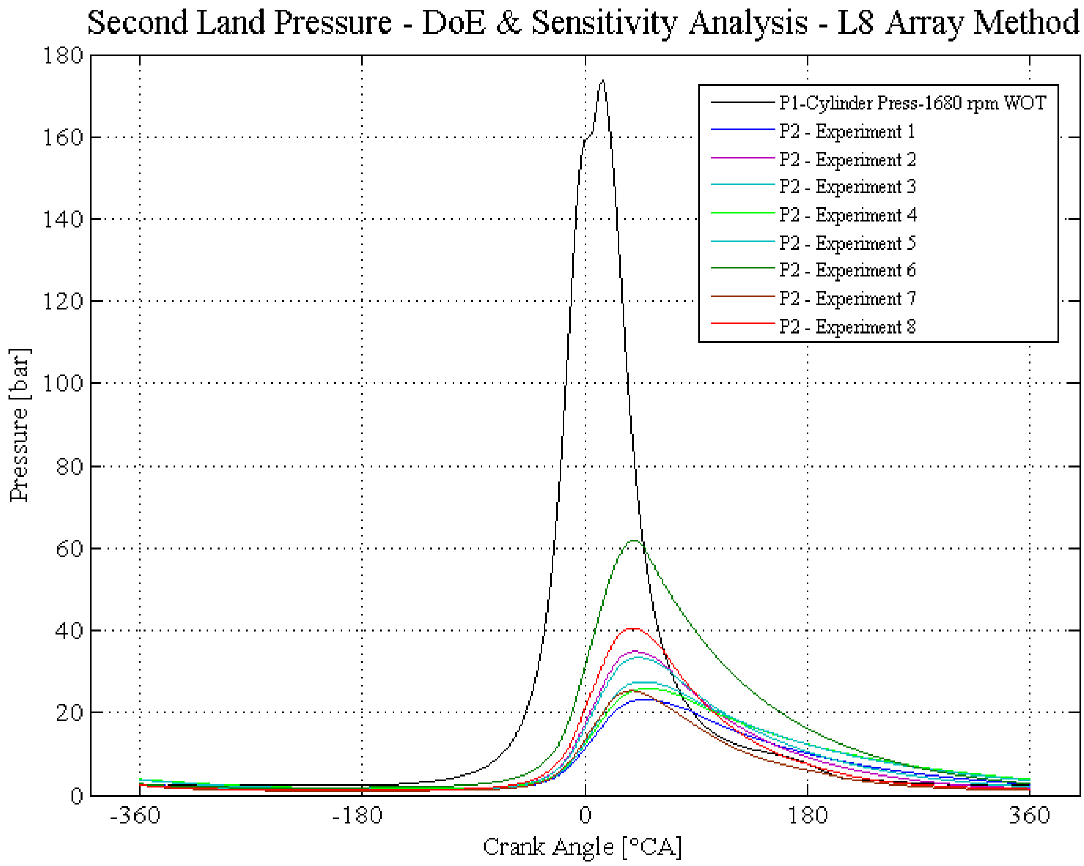

Figure 4.13 : Comparison of eight different ring pack configuration.

The next step in Taguchi method is to calculate the effects of the parameters according to the obtained results in Table 4.3. The program calculates the average pressure values in the minimum and maximum specification, then the difference will give us the severity of the effect for each selected parameters. That can be shown in an effect plot as in Figure 4.14. This plot is very useful to understand which parameters are most effective on second land pressures in which way.

The effect plot of design parameters on second land pressure has verified the findings in the previous sections. As it can be seen that the most effective parameters are first ring related dimensions which is the main source of the gas flow rate into the second land. With the increase of first ring end gap width, first ring height and discharge coefficient, the second land pressure will increase in parallel as the cross sectional area of flow is increased. It is shown that second ring related parameters are effective in reverse way as mentioned before. Additionally, the first ring/liner clearance value is not so effective as it is almost a straight line in the plot.

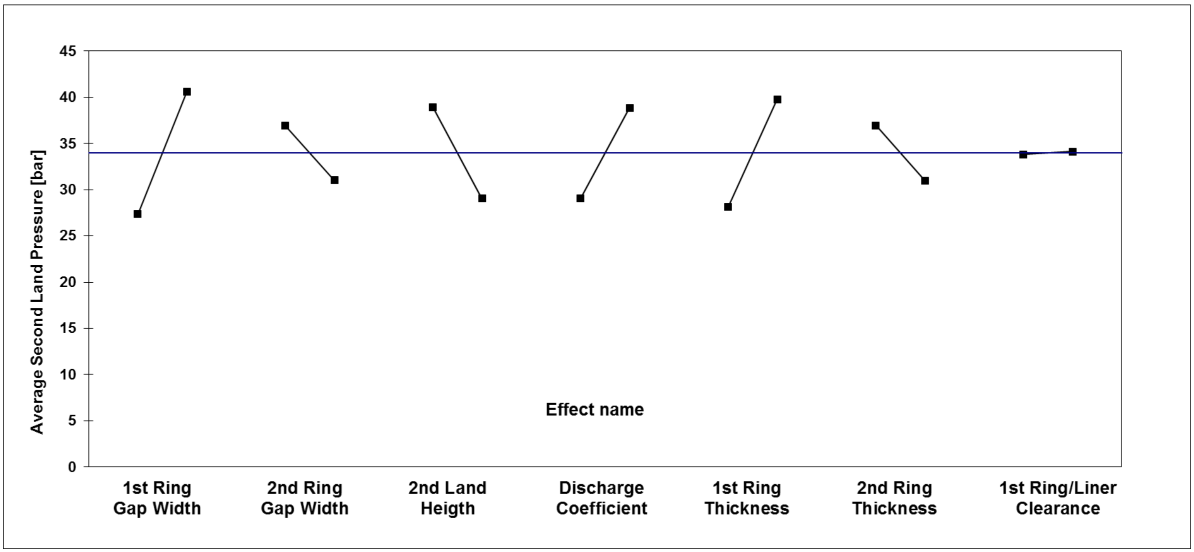

Figure 4.14 : Effect plot of design parameters on second land pressure.

The other option to be able to understand which parameter is most effective on second land pressure is to plot a “Half Normal Plot”.

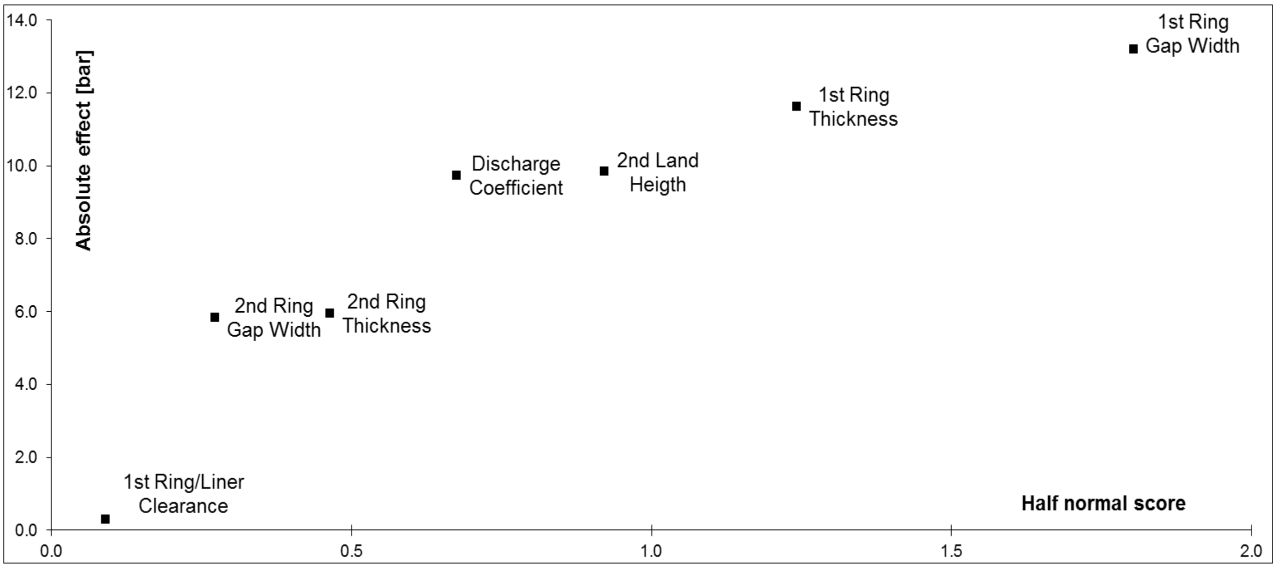

Figure 4.15 : Half normal plot of design parameters on second land pressure.

As it can be seen in Figure 4.15, the first ring design parameters (first ring gap width and first ring height) are effecting the inter ring pressures mostly.

4.4 Influence of Second Land Pressure on Friction Force

The second land pressure is a boundary condition with the combustion pressure which contributes to define the hydrodynamic pressure distribution between the ring surface and the cylinder liner. This will help to determine the minimum oil film thickness and the flooded area on the ring surface as well as the friction. Depending on the second land pressure value and the piston stroke direction, the cavitation point of the oil film may change. In case of oil film thickness falls below the lowest permissible limit and breaks down, a metal-metal contact during the stroke becomes possible. At that point, the friction will get higher due to asperity contact load increase on the effective ring areas.

In this section, three ring pack configurations have been chosen for the friction analysis according to the peak second land pressure values which obtained in sensitivity analysis before. The ring packs have been chosen as one of lowest, one of medium and one of highest second land pressure to be able to understand the effect of second land pressure on the friction and oil film thickness. The properties of selected ring packs are shown as in Table 4.4.

Table 4.4 : Selected ring packs for friction analysis

No	1st Ring Gap Width [mm]	2nd Ring Gap Width [mm]	2nd Land Height [mm]	Discharge Coefficient [-]	1st Ring Thick. [mm]	2nd Ring Thick. [mm]	1st Ring/Liner Clearance [mm]	Second Land Pressure [bar]
1	-	-	+	-	+	+	-	22,45
6	+	-	-	+	+	-	-	60,31
8	+	+	+	+	+	+	+	39,71

As mentioned before, it will be mainly focused on the effects of different second land pressures on the oil film thickness, oil film cavitation location, asperity contact load and oil film pressure. Those information can supply a useful information for a first prediction of the friction forces, wear levels due to asperity load and power losses due to frictional forces. With the implementation of the heat transfer from the cylinder walls and the piston secondary movement, the oil consumption calculations will be possible in the future. The second land pressure curves for selected ring packs are shown as in Figure 4.16.

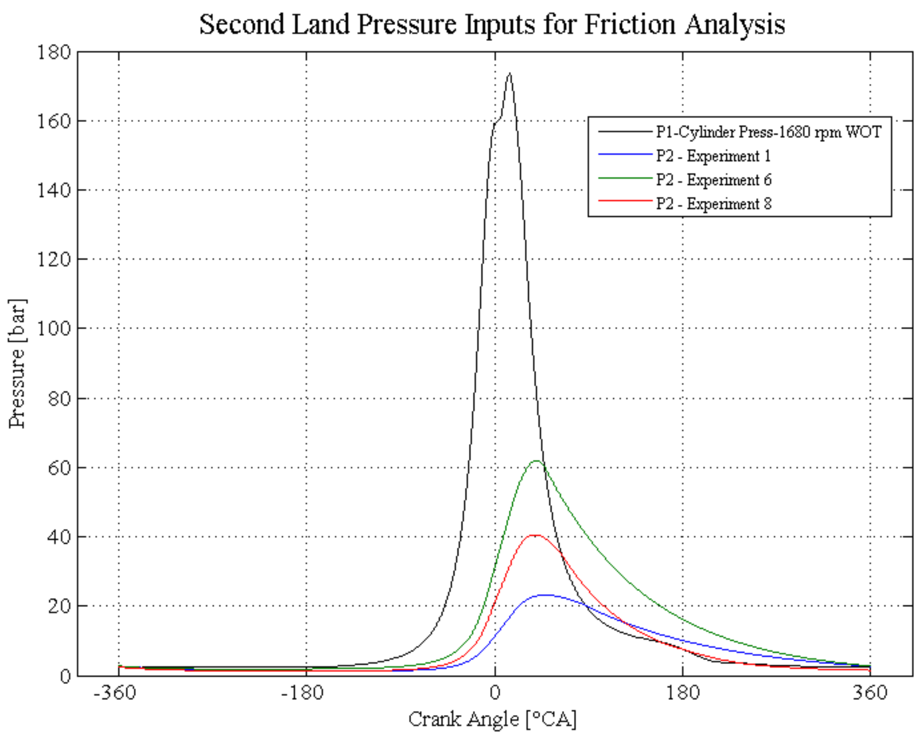

Figure 4.16 : Second land pressure inputs for friction analysis.

As mentioned before, it will be mainly focused on the effects of different second land pressures on the oil film thickness, oil film cavitation location, asperity contact load and oil film pressure. Those information can supply a useful information for a first prediction of the friction forces, wear levels due to asperity load and power losses due to frictional forces. With the implementation of the heat transfer from the cylinder walls and the piston secondary movement, the oil consumption calculations will be possible in the future.

4.4.1 Minimum Oil Film Thickness Comparison

For three different second land pressure, the resulted oil film thicknesses are shown in Figure 4.17.

The smallest oil film thickness has been observed at 14 °CA after TDC where the cylinder pressure is the highest for all ring packs. In this region, the velocity of the piston gets slow and the ring moves towards to the cylinder wall in the axial direction with the cylinder pressure acting on and behind it. This movement will be defined according to the magnitude of the second land pressure. At that point, lower second land pressure resulted with the smallest oil film thickness however the influence of pressure on the oil film thickness is very slight between configurations.

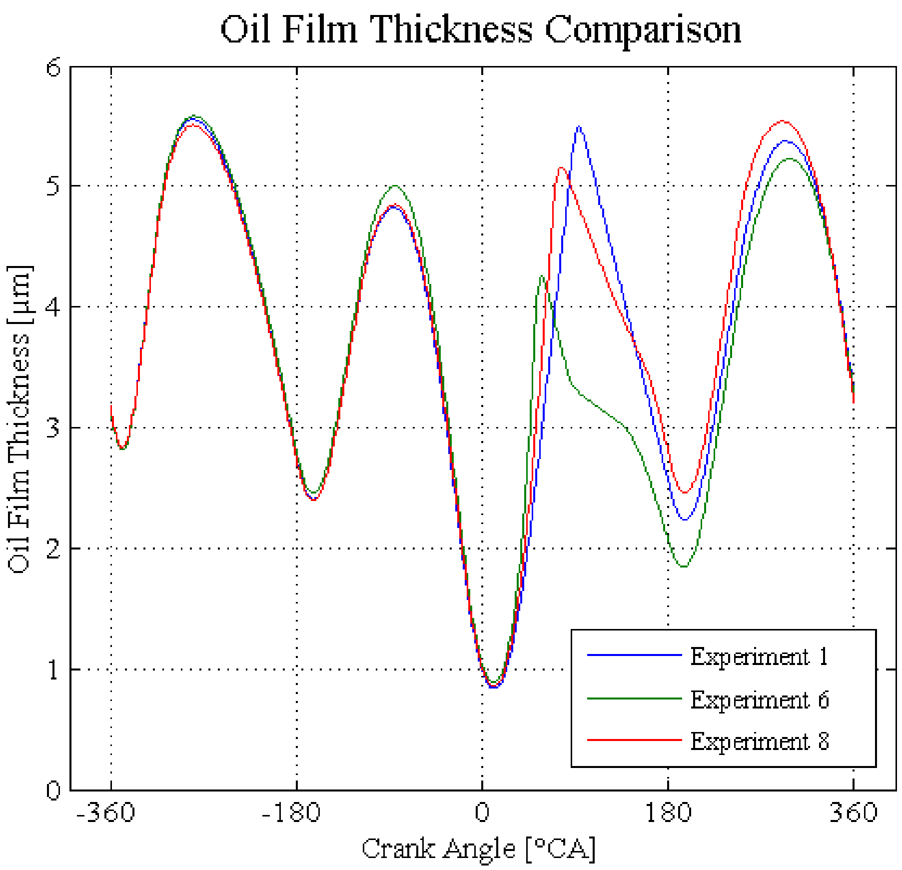

Figure 4.17 : Comparison of minimum oil film thickness.

No major differences have been seen during the intake and compression strokes as the second land pressures are very close to each other in that period.

As the pressure difference gets lower between cylinder and second land during the expansion, the difference becomes visible. Since the inter ring pressure is greater than combustion pressure in this region, piston ring leans to the upper groove flank and the inter ring pressure acts behind the ring. As the inter ring pressure of Experiment 6 is the greatest, the oil film thickness becomes minimum in that region.

During compression and early exhaust stroke, the combustion pressure acts behind the piston ring while the inter ring pressure acts in reverse on the non-lubricated surface of the piston ring. This reduces the thrust force and intends to lift the piston ring. As a result of this, the oil film thickness increases with Experiment 6 due to higher inter ring pressures.

In TDC region, the thrust forces decreases due to higher inter ring pressures with Experiment 6 which increases the oil film thickness slightly. In the aspect of cylinder wear, it can be considered that Experiment 6 is the most feasible condition.

4.4.2 Oil Film Cavitation Location Comparison

As an outlet boundary condition at the outlet of lubricant film, the second land pressure is an important parameter that defines the separation point of the lubricant from the ring. The element number "2000" shows the trailing edge of the piston ring.

Due to very minor second land pressure differences during the intake and compression stroke, the cavitation location is nearly same for all ring pack configurations.

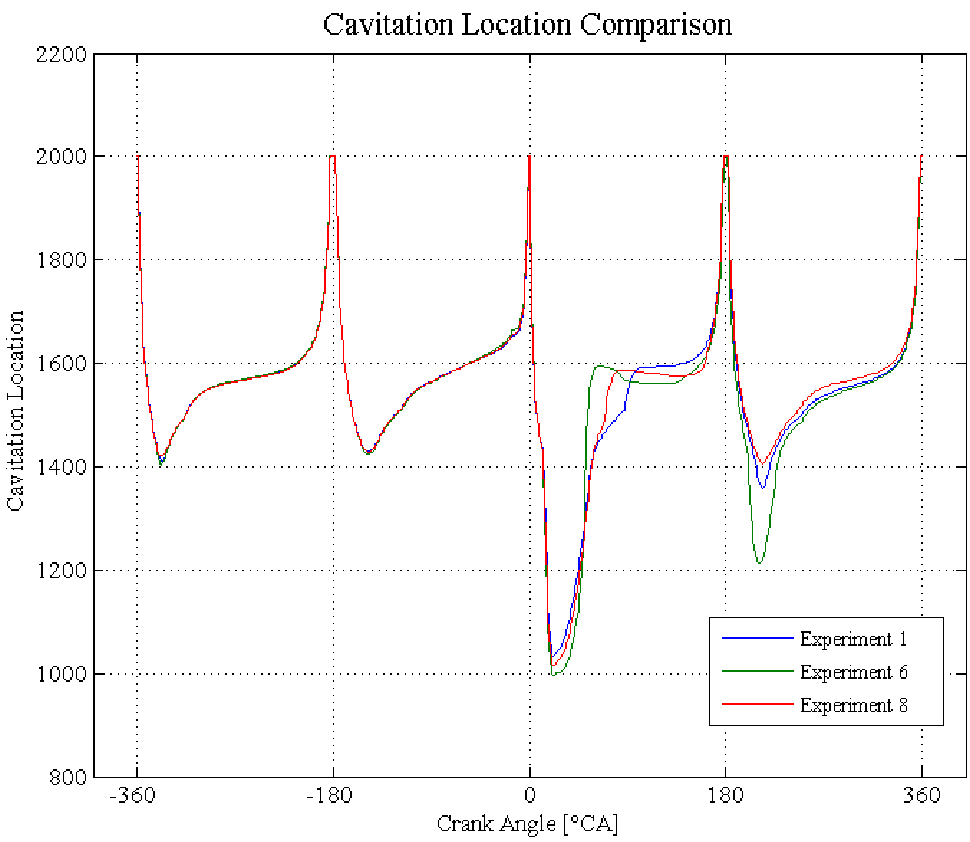

Figure 4.18 : Comparison of cavitation location.

During the combustion stroke where the Experiment 6 has the maximum second land pressure, the cavitation location goes to upwards to the inlet side of the ring. With the effect of increasing piston velocity during the expansion stroke, the cavitation location for all configurations start to move to the trailing edge of the ring again. And it can be seen that the cavitation point is still closer to the inlet boundary when the second land pressure is higher.

In addition to these, more controlled analysis need to be performed to be able to understand the effects of cavitation, pressure and shear flow as too many factors changes in the same time in this analysis.

4.4.3 Asperity and Oil Film Load Comparison

Asperity contact pressure comparison between the piston ring and the cylinder bore are shown in Figure 4.19. Asperity contact load is one of key parameters for the prediction of the cylinder wear levels. The wear patterns of a typical cylinder liner shows a high wear near TDC which agrees with the obtained results. At that point, the piston velocity is slow and little or no amount of lubricant is available. For all ring pack configurations, maximum asperity contact load has been observed near the top dead center when the combustion occurs which agrees with typical cylinder wear patterns.

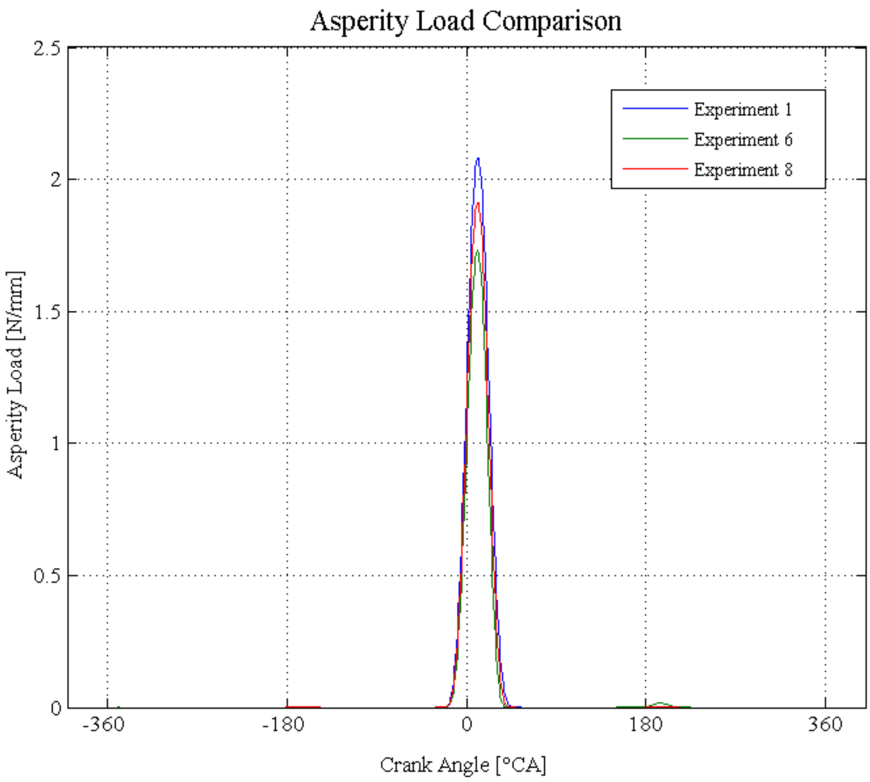

Figure 4.19 : Comparison of asperity contact load.

With smallest second land pressure obtained in Experiment 1, the greatest asperity contact load has been observed as the separation point of the oil film goes downwards and the pressure gradient gets larger which increases the load on the ring. During this stage, metal-to-metal contact with smaller second land pressure will be higher compared to the others which indicates that the cylinder wear level can be greater. During the other stages of engine cycle, the asperity contact load is almost zero as the hydrodynamic lubrication occurs for most of the stroke.

The oil film pressure distributions along the ring thickness as a function of crank angle degree and ring thickness are presented in Figure 4.20. As it can be seen from the diagrams, the maximum oil film pressure occurs in the inlet section of the ring near the top dead center where the cylinder pressure is the highest while it gets lower at the outlet section. At that point, no significant difference has been observed between the ring packs. However during the expansion stroke where the second land pressure is greater than combustion pressure, oil film load has increased in the same way with second land pressure.

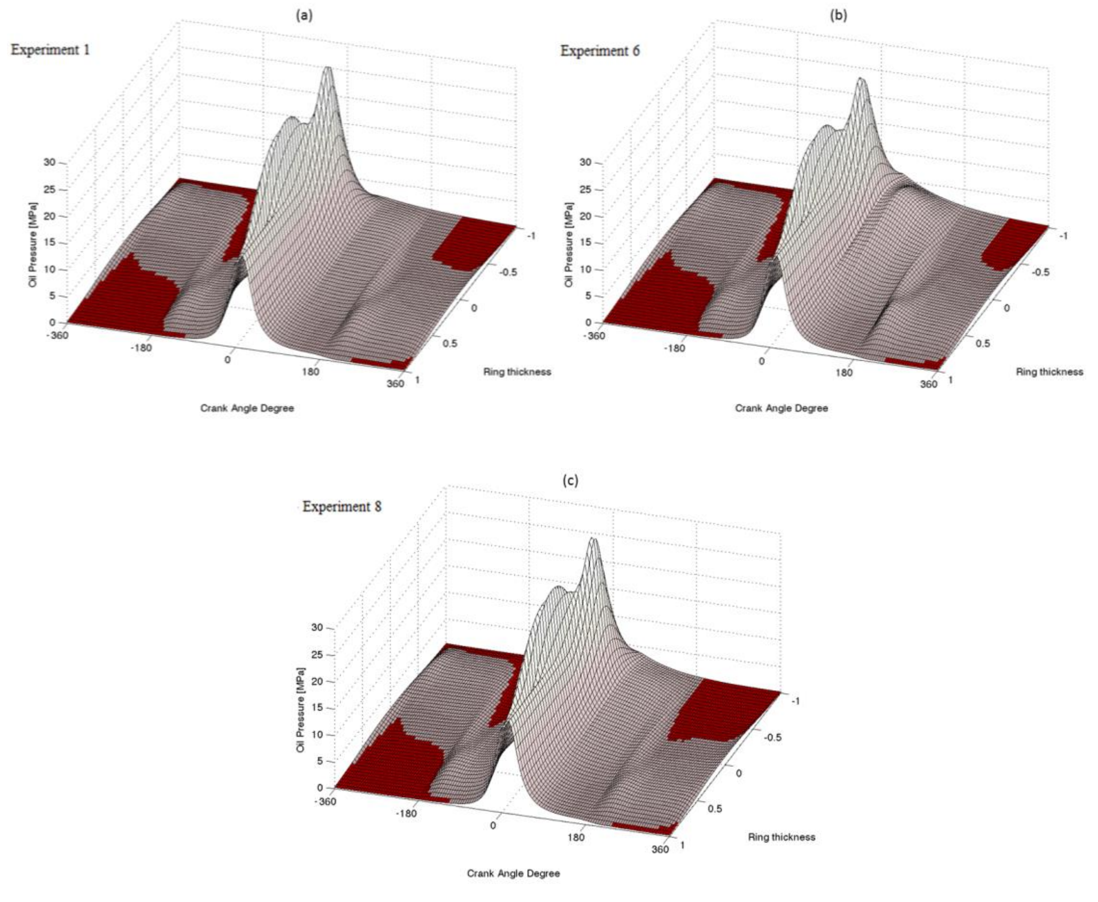

Figure 4.20 : Oil Pressure Distribution for Experiment 1, 6 and 8.

Red areas on the maps show where the cavitation occurs along the ring. At that time, the oil pressure is almost zero which means no oil is available. During the intake and compression strokes, this areas are almost same as the second land pressure figures are nearly equal to each other. On the other hand, this area gets larger with the reduction of pressure during the exhaust stroke.

4.4.4 Friction Force and Power Loss Comparison in First Compression Ring

The occurrence of the hydrodynamic lubrication for the most of the stroke has been shown in the previous sections. However, it is visible that there is a significant friction force increase near the top dead center due to high asperity load where the cylinder pressure and the normal load acting on a ring are high. When the second land pressure is lower, the cavitation location will be closer to the trailing edge of the ring which increases the pressure gradient acting on a ring. This will result with a higher load which contributes the friction force to be increased.

Friction force comparison and power loss comparison for three different ring pack configuration is presented in Figure 4.21 and Figure 4.22. It should be noted that this analysis has been carried out only for the first compression ring in one cylinder.

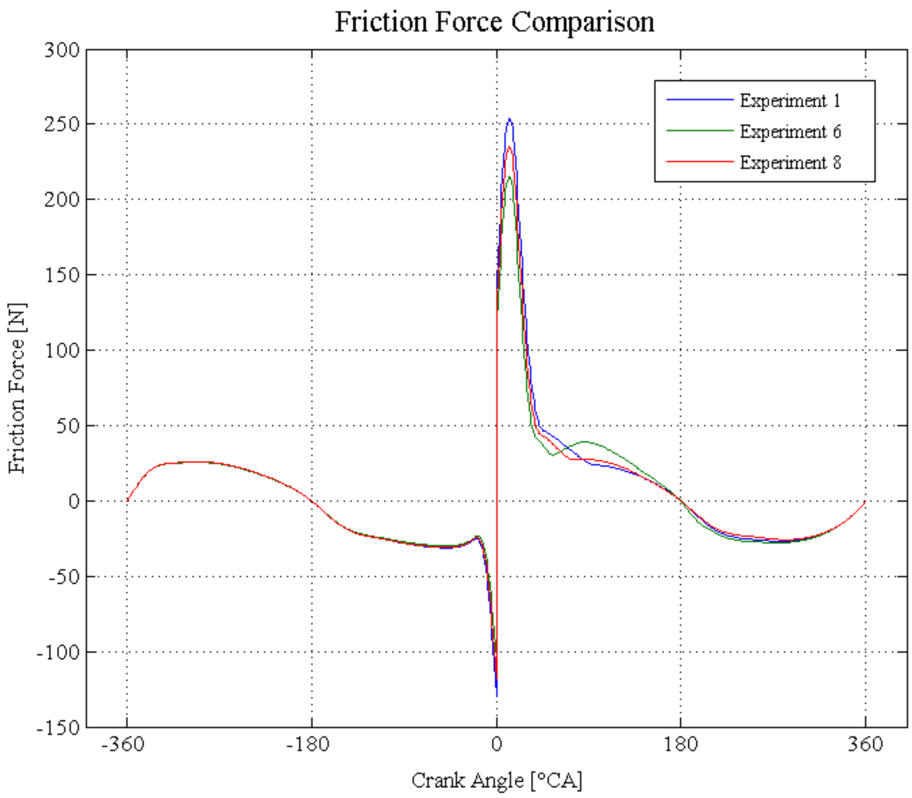

Figure 4.21 : Comparison of friction forces.

During the intake stroke, there is no visible difference between the ring pack configurations as the inter ring pressures are close to each other. During compression and early exhaust stroke, the oil film is thicker with Experiment 6 since higher inter ring pressure intends to lift the ring and reduces the thrust forces on the ring. As a result of this, the friction force is lower with Experiment 6 in that region.

During the late expansion and exhaust stroke, the inter ring pressure gets higher than the cylinder pressure and the piston ring moves towards to the upper side of the ring. The oil film thickness will be reduced due to higher inter ring pressures acting behind the ring which results an increase in the friction force.

The most important effect of the friction level of an engine is on the power losses which defines the performance of an engine. Power loss that caused by frictional forces is dependent on the friction force and the velocity of the piston. In this analysis, it is clearly seen that the power loss is increasing with the increase of the friction forces. Most of the loss of power occurs near the top dead center where the friction forces are the highest due to high asperity contact loads between the ring and liner.

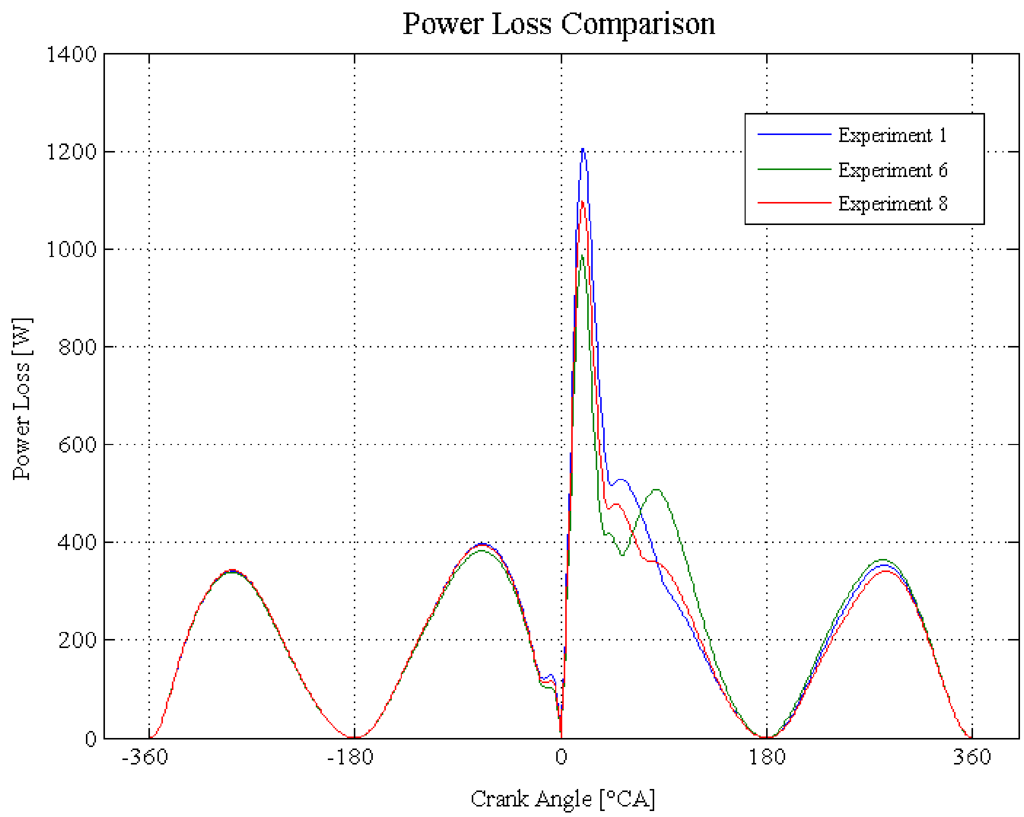

Figure 4.22 : Comparison of power loss.

The peak power loss has been observed near the top dead center with Experiment 1 ring pack which has the smallest second land pressure and the highest asperity load due to previously mentioned reasons.

The average values in Figure 4.22 have been calculated to be able to compare the average power losses between ring pack configurations. Table 4.5 shows the comparison between three ring pack configurations regarding average power losses during one engine cycle. With lower inter ring pressure configuration, highest power loss has been observed due to higher frictional forces.

Table 4.5 : Total power loss comparison during one engine cycle

Experiment No	Second Land Pressure	Power Loss (Avg)
#	**Bar**	**kW**
1	20	0,237
6	60	0,234
8	40	0,229

5. CONCLUSIONS AND RECOMMENDATIONS

Improving the fuel economy with decreasing the frictional losses and increasing the combustion efficiency is a challenge for the engine manufacturers due to satisfy the emission standards and customer expectations. With this purpose, the piston system is one of the first part of the engine that needs to be investigated in detailed since its many effects on the oil consumption, blow by and friction which is directly related with the engine power and fuel economy. The inter ring pressure is one of the most interested subject in the related piston ring dynamics literature so far as it defines the motion of the ring and the lubrication regime between running surface of the ring and liner that contributes a knowledge about an engine's important characteristics such as oil consumption, blow by and friction. In this study, specifically the pressure figures between top and second compression rings have been analysed with the aim of understanding the effect of the ring pack design parameters by conducting a sensitivity analysis via a statistical engineering method.

To summarize the work performed in this study:

- A deep literature research has been done to able to decide the nature of the work. Piston second land pressures were decided to be investigated regarding to the ring pack design parameter changes as this knowledge can be used to improve the piston ring dynamics understanding and help the engineers during design process.
- To predict the second land pressure mathematically, the previous related studies have been investigated which has shown that the "Volume-Orifice Method" was used mostly. It was decided to proceed with this method due to its reliability and accuracy.
- The study was a part of a measurement of second land pressures and friction project for 9.0L Ford ECOTORQ 380 PS engine. So the same engine has been chosen to be studied due to availability of the information about the engine parameters.

- According to the chosen engine design parameters, a labyrinth passage way scheme has been created to be able to model the gas flows.
- A computer code has been written in the MATLAB to calculate the gas flows and second land pressures. The code results have been verified with AVL Glide results which modelled for a previous study.
- The ring design parameters have been defined which was considered effective on the second land pressure. By changing the related geometrical or characteristical parameters, the MATLAB code has been run again and the results have been plotted for seven different factor.
- With the aim of understanding the effect of design parameters in together, a DoE matrix has been formed by using Taguchi Method. Eight experiments have been run in the MATLAB code for the eight different ring pack configurations. According to the results an “Effect Plot” has been plotted which showed the most effective parameter on the second land pressure.
- To understand the effect of the second land pressure on the friction and oil film thickness, three of results obtained in sensitivity analysis have been used in “Friction Calculation Code” which was written by Akalin and Newaz (2001).

The results obtained from the study in this thesis:

- With the nominal piston, ring and cylinder dimensions, the MATLAB model predicted the peak value of second land pressure as 32 bar at 1680 rpm WOT engine operating point which showed a good agreement with AVL Glide simulation results.
- First ring and second ring thickness and end gap width, piston second land height, orifice discharge coefficient and the ring/liner clearance have been investigated separately for minimum, nominal and maximum dimensions. It has been found out the most significant second land pressure changes occurred with the first ring related parameters’ modification.
- To be able to see the effect of all parameters in the same time, a DoE matrix has been created with Taguchi method which defines the most useful design configurations to compare. The output pressure values from this table varied

between 20 and 60 bars. The most effective three parameter on the inter ring pressure has been found out first ring end gap width, first ring thickness and piston second land height.

- The comparisons also showed that second land pressure had a direct proportion with first ring thickness, first ring gap width and ring discharge coefficient. As the increase of first ring and gap width will increase the flow rate into the second land with a greater cross sectional flow area.
- The second land pressure has an inverse proportion with the second ring height and gap width. Since the increasing of flow area of the second ring will cause the more gases to pass to the next chamber, it will cause a pressure drop in the second land volume. In addition, by increasing the volume of the second land by changing the second land height, the second land pressure has dropped because of the decreased number of gas particles in more expanded volume as a result of ideal gas law.
- The distance between ring and liner has been found out as not effective on the second land pressure which confirms the flow from this area was microscopic and negligible.
- Higher second land pressure which is the outlet boundary condition for the lubricant film moves the separation point of lubricant film towards to the inlet section of the piston ring.
- Change of cavitation location towards to the inlet section decreases the hydrodynamic pressure gradient on the ring. As a result of this, the asperity contact pressure decreases with the friction forces by the increase of second land pressures near the top dead center. At that point, it is observed a metal-to-metal contact which increases the cylinder liner wear.
- During compression and early expansion stroke, higher oil film thickness has been observed with higher inter ring pressures since it intends to lift the ring and reduces the thrust forces.
- During late expansion and exhaust stroke, with higher inter ring pressures than cylinder pressure, the piston ring leans on the upper flank of the groove and inter ring pressure acts behind the piston ring which pushes the ring

towards to the liner. As a result, highest inter ring pressure results with lowest oil film thickness which increases the friction.

- Friction force is directly influenced by the oil film thickness. In the regions where oil film thickness is lower, the friction force gets higher.
- Highest power loss has been observed with lowest inter ring pressure configuration due to increased friction levels.

This study is a first step for the modelling the gas flow through the piston ring system and determining the second land pressure. The results obtained during the study will be helpful and useful for the future piston system designs in the aspect of influence of the ring design parameters on the second land pressure.

In the future, the model can be improved by implementing the piston secondary movement, ring motion and cylinder bore deformations to be able to predict more and more accurate results. In addition to this, an oil consumption module can be added into the model with an appropriate heat transfer calculations.

Additionally, the understanding can be carried into the projects by conducting a more detailed sensitivity analysis by increasing the number of levels and parameters for optimizing the piston ring pack design.

On the other hand, real time second land pressure and friction measurement can be performed on the dynamometer which is an already on-going project to be able to verify the results with real world data.

REFERENCES

[1] **Ting, L. L. and Mayer, J.E.** (1974). Piston Ring Lubrication and Cylinder Bore Wear Analysis: Part 1 – Theory, *ASME J. Lubr. Technol*., **96**, pp. 305 – 314.

[2] **Ting, L. L. and Mayer, J.E.** (1974). Piston Ring Lubrication and Cylinder Bore Wear Analysis: Part 1 – Theory Verification, *ASME J. Lubr. Technol.*, **96**, pp. 258 – 266.

[3] **Rudy, B. L.; Dowson, D. and Economou, P. N.** (1981). The Prediction of Gas Pressures within the Ring Packs of Large Bore Diesel Engines, *Proc IMechE Part C: J Mechanical Engineering Sciences*, **23; 295C304**

[4] **Liu, Y. and Yongzhang, Y.** (1986). Prediction for the Sealing Characteristics of Piston Rings of a Reciprocating Compressor, *Proceedings of the International Compressor Engineering Conference at Purdue*, **Paper 583**, pp. 973 – 988.

[5] **Richardson, D. E.** (1996). Comparison of Measured and Theoretical Inter-Rıng Gas Pressure on a Diesel Engine, *SAE Technical Paper Series,* **961909**.

[6] **Tian, T.; Rabute, R.; Wong, W. Victor and Heywood, B. J** (1997). Effects of Piston-Ring Dynamics on Ring/Groove Wear and Oil Consumption in a Diesel Engine, *SAE Technical Paper Series*, **No.970835**.

[7] **Richardson, D.E. and Chen, J.** (2000). Predicted and Measured Ring Pack Performance of a Diesel Engine, *SAE Technical Paper Series,* **No. 2000-01-0918**.

[8] **Herbst, H.M. and Priebsch, H.H.** (2000). Simulation of Piston Ring Dynamics and Their Effect on Oil Consumption, *SAE Technical Paper Series,* **2000-01-1909**.

[9] **Richardson, D.E. and Krause, S.A** (2000). Predicted Effects of Cylinder Kit Wear on Blowby and Oil Consumption for Two Diesel Engines, Transactions of the *ASME, Journal of Engineering for Gas Turbines and Power,* **Vol.122**, October 2000, pages 520-525.

[10] **Tamminen, J.; Sandström, C. E. and Nurmi, H.** (2005). Influence of the Piston Inter-ring Pressure on the Ring Pack Behaviour in a Medium Speed Diesel Engine, *SAE Technical Paper Series*, **2005-01-3847**.

[11] **Mittler R.; Mierbach, A. and Richardson, D.** (2009 Understanding the fundamentals of Piston Ring Axial Motion and Twist and the Effects on Blow-By, *Proceedings of the ASME Internal Combustion Engine Division 2009 Spring Technical Conference,* **ICES2009-76080**.

[12] **Kolbenschmidt Service Tips & Infos** (2010). Oil Consumption and Oil Loss, 2nd Edition, **Article No. 50 003 605-02**, **ISBN 978-3-86522-219-0**.

[13] **Tian, T.** (1997) *Modeling the Performance of the Piston Ring-Pack in Internal Combustion Engines*, PhD. Thesis, Department of Mechanical Engineering, MIT.

[14] **Comfort, A.** (2003) An Introduction to Heavy-Duty Diesel Engine Frictional Losses and Lubricant Properties Affecting Fuel Economy – Part I, *SAE Technical Paper Series,* **2003-01-3225**.

[15] **AVL Excite User Guide** (2013) Piston Ring Dynamics and Lube Oil Consumption Module Theory, AVL List GmbH.

[16] **Arnault, N. and Bonne, S.** (2012) Engine Lube-Oil Consumption Stakes and Benefits from Significant Blow-by Oil Mist Reduction, *SAE Technical Paper,* **2012-01-1617**.

[17] **Yilmaz, E.; Tian, T.; Wong, V.W. and Heywood, J.B.** (2004) The Contribution of Different Oil Consumption Sources to Total Oil Consumption in a Spark Ignition Engine, *SAE Technical Paper Series*, **2004-01-2909**.

[18] **Freulund, K. and Yilmaz, E.** (2004) Impact of Engine Oil Consumption on Particulate Emissions, *ICAT: Future Automotive Technologies on Powertrain and Vehicle*, Istanbul, Turkey.

[19] **Akalin, O.** (2015) Automotive Tribology Lecture Notes, Department of Mechanical Engineering, ITU.

[20] **Gamble, R. J.; Priest, M.; Chittenden, R. J. and Taylor, C. M** (2000) Preliminary Study of the Influence of Piston Secondary Motion on Piston Ring Tribology, *Tribology Series,* **vol. 38**, pp. 679–691.

[21] **Gul, O.** (1997) *Real Time Oil Consumption Measurement of a Heavy Duty Diesel Engine*, MSc. Thesis, Department of Mechanical Engineering, ITU.

[22] **Akalin, O. and Newaz, G.M** (2001) Piston Ring-Cylinder Bore Friction Modeling in Mixed Lubrication Regime: Part I-Analytical Results, *Journal of Tribology 2001,* **Vol. 123**, pp 211-218.

[23] **Ford Otosan** (2005) FE Analysis Report, Internal Document

[24] **Url-1** < *http://korihandbook.federalmogul.com/en/section_39.htm* >, date retrieved 09.02.2015.

[25] **Url-2** < *https://www.dieselnet.com/tech/engine_crank.php*>, date retrieved 12.03.2015.

[26] **Url-3** < *http://courses.washington.edu/engr100/Section_Wei/* >, date retrieved 05.01.2015.

[27] **Url-4** < *https://controls.engin.umich.edu*>, date retrieved 10.04.2015.

CURRICULUM VITAE

Name Surname: Ahmet Ebrinç

Place and Date of Birth: Keçiören, 12 – 09 – 1988

E-Mail: aebrinc1@ford.com, aebrinc@gmail.com

B.Sc.: Yıldız Technical University, Mechanical Engineering, 2011

Professional Experience:

Engine test and design verification engineer at Ford Otosan Product Development since August 2011.